

On the role of the $\Delta(1232)$ on the transverse nuclear response in the (e, e') reaction.

E. Bauer*

Departamento de Física, Facultad de Ciencias Exactas,
Universidad Nacional de La Plata, La Plata, 1900, Argentina.

October 16, 2018

Abstract

The transverse nuclear response to an electromagnetic probe which is limited to create (or destroyed) a particle-hole (ph) or delta-hole (Δh) pair is analyzed. Correlations of the random phase approximation (RPA) type and self energy insertions are considered. For RPA correlations we have developed a scheme which includes explicitly the Δ and the exchange terms. Self energy insertions over ph and Δh bubbles are studied. Several residual interactions based on a contact plus a $(\pi + \rho)$ -meson exchange potential are used. All calculations are performed in non-relativistic nuclear matter. The main effect of the Δ is to reduce the intensity over the nuclear quasi-elastic peak. Exchange RPA terms are very important, while the self energy depends strongly on the residual interaction employed. We compare our final result with data for ^{40}Ca at momentum transfer $q = 410$ and $q = 550$ MeV/c.

PACS number: 21.65, 25.30.Fj, 21.60.Jz.

Keywords: Nuclear Electron Scattering. Delta resonance.

*Fellow of the Consejo Nacional de Investigaciones Científicas y Técnicas, CONICET.

1 Introduction.

Quasi elastic electron scattering is a powerful tool to study the atomic nucleus. Since the experimental separation of the inclusive longitudinal and transverse response function [1]-[4], a great deal of theoretical effort was developed to understand these responses. More recently [5], the extraction of the experimental points was re-analyzed. Even though, till now there is no theoretical frame which is able to account for both longitudinal and transverse response functions at any momentum transfer.

Let us resume some of the theoretical efforts. Some works assume that the nucleus is described by a Fermi gas with a modified charge radius for individual nucleons [6]. But much of the works are based on a many body theory [7]-[29]. The present work belongs to this second group. Within this group some works deal with relativistic effects [7], the correlated basis function [8], meson exchange currents (MEC) [9], [11]-[13], RPA correlations [14]-[18], Second RPA [19, 20], Extended RPA [21]-[23], the Green function approach [24], and the Δ degree of freedom [25]-[29]. In fact this list is not complete, we just wanted to mention the most relevant approaches related with the present work. From all these references, we learn that each effect which is considered in them, is important. In addition, there is a strong dependence on the residual interaction employed. The residual interaction is usually picked from the literature, which in general corresponds to a parameterization fixed for low energy calculations. This procedure is questionable because an effective interaction depends on the theory where it was adjusted [18, 27, 29].

That means that the search for one simple mechanism to explain data seems to be hopeless. Many correlations like RPA, MEC, the Δ degree of freedom and so on, are all equally important. Also, the nuclear residual interaction is unknown. Fortunately, some simplification occurs as non relativistic nuclear matter describe reasonable well the properties of medium mass nuclei in the energy momentum region of interest, once a proper Fermi momentum is used [13].

The delta play an important role in the transverse nuclear response. In this work we have developed a method to account for RPA correlations with the explicit inclusion of the Δ degree of freedom and we have also analyzed self energy insertions. This is done for several residual interactions. As mentioned, these contributions should be seen as part of a set of calculations which aim should be to reproduce both

the longitudinal and the transverse responses.

The paper is organized as follows. In Section 2 we present the formalism for RPA and self energy insertions which includes the Δ . In Section 3, we make a numerical analysis of the different contributions. Finally, Section 4 contains the conclusions.

2 Formalism

In this section we will show first the nuclear response to an external electromagnetic probe in a general way. Then in two sub-sections RPA correlations and final state interactions (FSI) of the self-energy type will be analyzed in detail.

Let us start by introducing the nuclear response function as,

$$R(\mathbf{q}, \hbar\omega) = -\frac{1}{\pi} \text{Im} < |\mathcal{O}^\dagger G(\hbar\omega) \mathcal{O}| >, \quad (1)$$

where \mathbf{q} represents the magnitude of the three momentum transfer by the electromagnetic probe, $\hbar\omega$ the excitation energy and $| >$ is the Hartree-Fock nuclear ground state. Ground state correlations beyond RPA are not analyzed in this work. The polarization propagator is given by,

$$G(\hbar\omega) = \frac{1}{\hbar\omega - H + i\eta} - \frac{1}{\hbar\omega + H - i\eta}, \quad (2)$$

where H is the nuclear Hamiltonian. As usual, H is separated into a one-body part, H_0 , and a residual interaction V . In Eq. (1) \mathcal{O} represents the external probe, given by a one body excitation operator which will be defined soon.

We present now two projection operators P and Q . The action of P is to project into the ground state, the one particle-one hole (ph) and one delta-one hole (Δh) configurations. While Q projects into the residual n_p particle- n_h hole- n_Δ delta configurations. More explicitly,

$$P = | > < | + P_N + P_\Delta, \quad (3)$$

with

$$P_N = \sum_{ph} |ph><ph|, \quad (4)$$

$$P_\Delta = \sum_{\Delta h} |\Delta h><\Delta h| \quad (5)$$

and

$$Q = \sum_{\substack{n_h \geq 2 \\ 0 \leq n_p \leq n_h}} |n_p p (n_h - n_p) \Delta n_h h > < n_p p (n_h - n_p) \Delta n_h h|, \quad (6)$$

where we have introduced P_N and P_Δ for convenience. It is easy to verify that $P + Q = 1$, $P^2 = P$, $Q^2 = Q$, and $PQ = QP = 0$ and also, $P_i P_j = \delta_{ij} P_i$ and $P_i Q = Q P_i = 0$ ($i = N, \Delta$).

By inserting the identity into eq. (1) and noting that the external one body operator can connect the Hartree-Fock ground state only to the P space, we have,

$$R_{PP}(\mathbf{q}, \hbar\omega) = -\frac{1}{\pi} \text{Im} < \mathcal{O}^\dagger P G_{PP}(\hbar\omega) P \mathcal{O} >, \quad (7)$$

where $G_{PP} \equiv PGP$. It is easy to see that,

$$G_{PP}(\hbar\omega) = \frac{1}{\hbar\omega - H_{PP} - \Sigma^{PQP} + i\eta} - \frac{1}{\hbar\omega + H_{PP} + \Sigma^{PQP} - i\eta}, \quad (8)$$

where,

$$\Sigma^{PQP} = V_{PQ} \frac{1}{\hbar\omega - H_{QQ} + i\eta} V_{QP} - V_{PQ} \frac{1}{\hbar\omega + H_{QQ} - i\eta} V_{QP}, \quad (9)$$

with obvious definitions for H_{PP} , etc. As our main concern is the effect of the $\Delta(1232)$, we analyze the nuclear transverse response. The matrix elements for the external operator are then [30],

$$< ph | \mathcal{O} | > = G_E(\mathbf{q}, \hbar\omega) \frac{i}{2mq} \frac{\mu_s + \mu_v \tau_3}{2} \mathbf{q} \times (\boldsymbol{\sigma} \times \mathbf{q}) \quad (10)$$

and

$$< \Delta h | \mathcal{O} | > = G_\Delta(\mathbf{q}, \hbar\omega) \frac{i}{2mq} \mu_{N\Delta} T_3 \mathbf{q} \times (\mathbf{S} \times \mathbf{q}) \quad (11)$$

where m is the nucleonic mass, we have used $\mu_s = 0.88$, $\mu_v = 4.70$ and $\mu_{N\Delta} = 3.756$. In eq. (10) we have neglected the convection contribution. In eq. (11) the Pauli matrices $\boldsymbol{\sigma}$ and τ_3 were replaced by the corresponding transitions matrices \mathbf{S} and T_3 [31]. The electromagnetic form factors are,

$$G_E(\mathbf{q}, \hbar\omega) = (1 + \frac{(\hbar cq)^2 - (\hbar\omega)^2}{(839 \text{MeV})^2})^{-2}. \quad (12)$$

$$G_\Delta(\mathbf{q}, \hbar\omega) = (1 + \frac{(\hbar cq)^2 - (\hbar\omega)^2}{(1196 \text{MeV})^2})^{-2} (1 + \frac{(\hbar cq)^2 - (\hbar\omega)^2}{(843 \text{MeV})^2})^{-1/2}. \quad (13)$$

The residual interaction in the ph sector is given by,

$$V(l) = \frac{f_{\pi NN}^2}{\mu_\pi^2} \Gamma_{\pi NN}^2(l) (g_{NN} \boldsymbol{\sigma} \cdot \boldsymbol{\sigma}' + \tilde{g}'_{NN}(l) \boldsymbol{\tau} \cdot \boldsymbol{\tau}' \boldsymbol{\sigma} \cdot \boldsymbol{\sigma}' + \tilde{h}'_{NN}(l) \boldsymbol{\tau} \cdot \boldsymbol{\tau}' \boldsymbol{\sigma} \cdot \hat{\boldsymbol{l}} \boldsymbol{\sigma}' \cdot \hat{\boldsymbol{l}}) \quad (14)$$

with

$$\tilde{g}'_{NN}(l) = g'_{NN} - \frac{\Gamma_{\rho NN}^2(l)}{\Gamma_{\pi NN}^2(l)} C_{\rho NN} \frac{l^2}{l^2 + \mu_\rho^2}, \quad (15)$$

$$\tilde{h}'_{NN}(l) = -\frac{l^2}{l^2 + \mu_\pi^2} + \frac{\Gamma_{\rho NN}^2(l)}{\Gamma_{\pi NN}^2(l)} C_{\rho NN} \frac{l^2}{l^2 + \mu_\rho^2}, \quad (16)$$

where $\mu_\pi \hbar c$ ($\mu_\rho \hbar c$) is the pion (rho) rest mass and the Landau Migdal parameters g_{NN} and g'_{NN} account for short range correlations. We have used the static limit for the interaction, where l represents the momentum transfers. For the form factor of the πNN (ρNN) vertex we have taken

$$\Gamma_{\pi NN, \rho NN}(l) = \frac{\Lambda_{\pi NN, \rho NN}^2 - (\mu_{\pi, \rho} \hbar c)^2}{\Lambda_{\pi, \rho}^2 + (\hbar c l)^2}, \quad (17)$$

Numerical values for the coupling constants, masses and form factors will be given in the next section. Analogous expressions are obtained when deltas are involved. In this case no Landau Migdal g parameter is considered. All the other NN constants and parameters should be replace by their corresponding $N\Delta$ and $\Delta\Delta$ values. Also Pauli matrices must be replaced by the corresponding transitions matrices \mathbf{S} and \mathbf{T} or \mathbf{s} and $\mathbf{\mathcal{T}}$, the 3/2-3/2 spin matrices (see ref. [27]); depending on the character of the mesonic vertex. Just as an example, we consider the interaction where in one mesonic vertex there is an incoming and outgoing Δ and in the other vertex there is a hole. In that case the interaction reads,

$$V'(l) = \frac{f_{\pi NN} f_{\pi \Delta \Delta}}{\mu_\pi^2} \Gamma_{\pi NN}(l) \Gamma_{\pi \Delta \Delta}(l) (\tilde{g}'_{\Delta \Delta}(l) \boldsymbol{\tau} \cdot \mathbf{\mathcal{T}} \boldsymbol{\sigma} \cdot \mathbf{S} + \tilde{h}'_{\Delta \Delta}(l) \boldsymbol{\tau} \cdot \mathbf{\mathcal{T}} \boldsymbol{\sigma} \cdot \hat{\boldsymbol{l}} \mathbf{S} \cdot \hat{\boldsymbol{l}}) \quad (18)$$

Equations (7)-(9) generates the standard RPA and self energy contributions. We analyze separately now these two kind of correlations.

2.1 RPA correlations:

The aim of this subsection is to present a RPA formalism in nuclear matter with the $\Delta(1232)$ and which explicitly includes exchange terms. As a first step we neglect self

energy insertions (or equivalently we turn off the Q -space). Eq. (8) becomes,

$$G_{PP}(\hbar\omega) = \frac{1}{\hbar\omega - H_0 - V + i\eta} - \frac{1}{\hbar\omega + H_0 + V - i\eta}, \quad (19)$$

where we have split the nuclear Hamiltonian. The presence of V , the residual interaction, makes G_{PP} to be nondiagonal in P -space. To treat this, the standard Dyson equation is employed,

$$\begin{aligned} G_{PP} &= G_{PP}^0 + G_{PP}^0 V G_{PP} \\ &= G_{PP}^0 + G_{PP}^0 V G_{PP}^0 + G_{PP}^0 V G_{PP}^0 V G_{PP}^0 + \dots, \end{aligned} \quad (20)$$

where G_{PP}^0 results from replacing the total Hamiltonian by its one body part. Eq. (20) contains both direct and exchange terms. If one keeps only direct terms or if one uses a contact interaction, then Eq. (20) can be easily sum up to infinite order, leading to the ring series. This sum can not be done when exchange terms for a finite range interaction are included. Even this is a well known fact, let us show it in a rather elementary way, as it will simplify the further discussion.

We consider the first two terms in the second line of Eq. (20) and we replace P by its definition of Eq. (3). In addition, let us analyze ph configurations only. Taking the matrix elements for the first perturbative terms and inserting them into Eq. (7), the response function becomes,

$$\begin{aligned} R_{PP} &= -\frac{1}{\pi} \text{Im} \left\{ \sum_{ph} \langle \mathcal{O}^\dagger | ph \rangle \langle ph | G^0 | ph \rangle \langle ph | \mathcal{O} \rangle + \right. \\ &\quad \sum_{ph, p'h'} \langle \mathcal{O}^\dagger | ph \rangle \langle ph | G^0 | ph \rangle \langle ph | V | p'h' \rangle_{D+E} \times \\ &\quad \left. \langle p'h' | G^0 | p'h' \rangle \langle p'h' | \mathcal{O} \rangle + \dots \right\}. \end{aligned} \quad (21)$$

using momentum conservation as shown in Fig. 1, direct and exchange matrix elements of the residual interaction can be drawn as,

$$\langle (\mathbf{h} + \mathbf{q}), \mathbf{h} | V | (\mathbf{h}' + \mathbf{q}'), \mathbf{h}' \rangle_D \equiv \mathcal{V}_D(q) \quad (22)$$

and

$$\langle (\mathbf{h} + \mathbf{q}), \mathbf{h} | V | (\mathbf{h}' + \mathbf{q}'), \mathbf{h}' \rangle_E \equiv \mathcal{V}_E(|\mathbf{h} - \mathbf{h}'|). \quad (23)$$

Finally, the response function becomes,

$$\begin{aligned}
R_{PP} = & -\frac{1}{\pi} \text{Im} \left\{ \sum_{ph} \langle \mathcal{O}^\dagger | ph \rangle \langle ph | G^0 | ph \rangle \langle ph | \mathcal{O} \rangle \right\} + \\
& \left(\sum_{ph} \langle \mathcal{O}^\dagger | ph \rangle \langle ph | G^0 | ph \rangle \right) \mathcal{V}_D(q) \\
& \left(\sum_{p'h'} \langle p'h' | G^0 | p'h' \rangle \right) \langle p'h' | \mathcal{O} \rangle + \\
& \sum_{ph, p'h'} \langle \mathcal{O}^\dagger | ph \rangle \langle ph | G^0 | ph \rangle \mathcal{V}_E(|\mathbf{h} - \mathbf{h}'|) \\
& \langle p'h' | G^0 | p'h' \rangle \langle p'h' | \mathcal{O} \rangle + \dots \}. \tag{24}
\end{aligned}$$

it is trivial to extend the procedure to higher orders or Δh configurations. As seen in the second term of this equation, direct terms split into common factors. This is not the case of the third term due to the presence of $\mathcal{V}_E(|\mathbf{h} - \mathbf{h}'|)$, except if one uses a contact interaction ¹.

Exchange terms of the RPA type happens to be important (see refs. [16] and [17]) and as shown, they can not be sum up to infinite order. One has to evaluate each exchange term explicitly and in practice this can be done up to second order. In the next section, we will show that keeping exchange terms up to second order is not in general a good approximation. Evidently if one choose an arbitrarily small residual interaction a fast convergence to the RPA series will be obtained from its firsts perturbative terms.

Let us go back to our scheme which accounts for RPA correlations in nuclear matter with the explicit inclusion of exchange terms. The scheme is an extension of the one developed in ref. [17] to include Δh excitations and it is based on three elements. First, it is possible to sum up to infinite order exchange terms for a contact interaction. Second, it is possible to sum up to infinite order direct terms for any interaction and for some particular interactions the first two perturbative terms accounts for the full sum. Finally, even the exchange terms of a finite range interaction

¹Also the same holds when $\mathcal{V}_E(|\mathbf{h} - \mathbf{h}'|)$ is a separable interaction which is not the case of a $(\pi + \rho)$ -meson exchange potential.

can be evaluated up to second order, it is plausible to expect that higher order terms will be negligible small if it is the case for theirs corresponding direct ones and they keep smaller than them.

Thus, we divide the residual interaction as follows,

$$V = V_1 + V_2, \quad (25)$$

where V_1 is a contact interaction and V_2 contains a contact plus the exchange of the $(\pi + \rho)$ -mesons (or any finite range interaction). The contact term in V_2 is chosen to fulfill the second and third conditions mentioned above. An additional constrain is that the remaining contact term (V_1) allows a perturbative treatment.

The polarization propagator of Eq. (19) can now be written as

$$G_{PP} = G_{1PP} + G_{2PP} + G_{12PP}, \quad (26)$$

where,

$$G_{1PP} = G_{PP}^0 + G_{PP}^0 V_1 G_{1PP}, \quad (27)$$

$$G_{2PP} = G_{PP}^0 V_2 G_{PP}^0 + G_{PP}^0 V_2 G_{PP}^0 V_2 G_{PP}^0, \quad (28)$$

$$G_{12PP} = G_{PP}^0 V_2 G_{PP}^0 V_1 G_{PP}^0 + G_{PP}^0 V_2 G_{PP}^0 V_1 G_{PP}^0 V_1 G_{PP}^0 + \dots \quad (29)$$

Inserting now Eq. (26) into Eq. (7) one can define three different contributions to the response function, R_1 , R_2 and R_{12} , associated to G_1 , G_2 and G_{12} , respectively. Let us analyzed each contribution separately.

The R_1 contribution is simply the ring approximation (RA), with the inclusion of the Δh space. The solution of Eq. (27) is given by (see Ref. [25] and [32]),

$$G_{1PP} = (I - G_{PP}^0 V_{1PP})^{-1} G_{PP}^0, \quad (30)$$

where

$$G_{PP}^0 = \begin{pmatrix} G_{NN}^0 & 0 \\ 0 & G_{\Delta\Delta}^0 \end{pmatrix}, \quad V_{1PP} = \begin{pmatrix} V_{1NN} & V_{1\Delta N} \\ V_{1N\Delta} & V_{1\Delta\Delta} \end{pmatrix} \quad (31)$$

and

$$I = \begin{pmatrix} P_N & 0 \\ 0 & P_\Delta \end{pmatrix}. \quad (32)$$

We have split up the projection operator into its components P_N and P_Δ . Finally, the contact contribution to the response becomes,

$$R_1(\mathbf{q}, \hbar\omega) = -\frac{1}{\pi} \text{Im} \langle | (\mathcal{O}^\dagger_N, \mathcal{O}^\dagger_\Delta) \begin{pmatrix} G_{1NN} & G_{1\Delta N} \\ G_{1N\Delta} & G_{1\Delta\Delta} \end{pmatrix} \begin{pmatrix} \mathcal{O}_N \\ \mathcal{O}_\Delta \end{pmatrix} | \rangle \quad (33)$$

where we have defined $\mathcal{O}_N = \langle ph | \mathcal{O} | \rangle$ and $\mathcal{O}_\Delta = \langle \Delta h | \mathcal{O} | \rangle$.

As mentioned V_1 is a contact interaction and contains both direct and exchange contributions. How to build this direct plus exchange interaction is described in Appendix A. Obviously Eq. (33) is also valid for direct terms of any interaction. A graphical representation of the firsts perturbative terms stemming from this equation is given in Fig. 2.

Also in Fig. 2 we show the R_2 contribution. In Appendix B, we list analytical expressions for the main terms contributing to R_2 , given by the standard rules for Golstone diagrams.

Finally, also some of the lower order contributions to R_{12} are presented in Fig. 2. In our scheme V_2 is included up to second order and V_1 up to infinite order. From the three contributions, R_{12} has the most complex structure. Formally, the analysis is simplified due to the fact that a direct plus exchange contact interaction can not connect the P_N and P_Δ spaces (see Appendix A).

In Fig. 3 we show in detail the contributions to R_{12} limiting V_2 up to first order. It was further split up into three contributions, $(R_{12})_{NN}$, $(R_{12})_{N\Delta}$ and $(R_{12})_{\Delta\Delta}$; depending on the configuration where the external operator is attached. Each line in Fig. 3 represents a sum up to infinite order in V_1 . Let us call by x the ph bubble and by z the corresponding Δh one. Both are defined in Appendix B. Also we denote by B_{1NN} , $B_{1N\Delta}$ and $B_{1\Delta\Delta}$ (B_{2NNN} , $B_{2NN\Delta}$, $B_{2N\Delta\Delta}$ and $B_{2\Delta\Delta\Delta}$) the direct plus exchange response functions which are first order in V_2 (second order in V_2). In each case, subindex N or Δ refers to the particular P space which builds the contribution. For instance, B_{1NN} is the sum of graphs $(B_{1NN})_D$ plus $(B_{1NN})_E$ of Fig. 1. Expressions for each of these contributions are given in Appendix B.

We show now R_{12} . As mentioned,

$$R_{12} = (R_{12})_{NN} + (R_{12})_{N\Delta} + (R_{12})_{\Delta\Delta}, \quad (34)$$

where,

$$(R_{12})_{NN} = -\frac{1}{\pi} \text{Im} \left\{ \frac{1}{2} \mathcal{V}'_{1N} (B_{1NN} + 3 B_{2NNN}) \frac{x (2 - \mathcal{V}'_{1N} x)}{(1 - \mathcal{V}'_{1N} x)^2} \right\}, \quad (35)$$

$$\begin{aligned} (R_{12})_{N\Delta} &= -\frac{1}{\pi} \text{Im} \left\{ \mathcal{V}'_{1N} \mathcal{V}'_{1\Delta} [B_{1N\Delta} \left(\frac{1}{1 - \mathcal{V}'_{1N} x} \frac{1}{1 - \mathcal{V}'_{1\Delta} z} - 1 \right) + \right. \\ &\quad + B_{2NN\Delta} \frac{x (2 - \mathcal{V}'_{1N} x)}{(1 - \mathcal{V}'_{1N} x)^2} \frac{1}{1 - \mathcal{V}'_{1\Delta} z} + \\ &\quad \left. + B_{2N\Delta\Delta} \frac{z (2 - \mathcal{V}'_{1\Delta} z)}{(1 - \mathcal{V}'_{1\Delta} z)^2} \frac{1}{1 - \mathcal{V}'_{1N} x} \right\}, \end{aligned} \quad (36)$$

$$(R_{12})_{\Delta\Delta} = -\frac{1}{\pi} \text{Im} \left\{ \frac{1}{2} \mathcal{V}'_{1\Delta} (B_{1\Delta\Delta} + 3 B_{2\Delta\Delta\Delta}) \frac{z (2 - \mathcal{V}'_{1\Delta} z)}{(1 - \mathcal{V}'_{1\Delta} z)^2} \right\} \quad (37)$$

and

$$\mathcal{V}'_{1N} = 8 \frac{mc^2}{(2\pi)^2} \frac{f_{\pi NN}^2}{4\pi} \frac{1}{\mu_\pi^2 k_F} g'_{1NN} \Gamma_{\pi NN}^2(Q) \quad (38)$$

$$\mathcal{V}'_{1\Delta} = \frac{32}{9} \frac{mc^2}{(2\pi)^2} \frac{f_{\pi\Delta N}^2}{4\pi} \frac{1}{\mu_\pi^2 k_F} g'_{1\Delta\Delta} \Gamma_{\pi\Delta N}^2(Q) \quad (39)$$

where g'_{1NN} and $g'_{1\Delta\Delta}$ are the Landau Migdal direct plus exchange terms for the contact interaction V_1 . Some third order contributions ($B_{2N\Delta N}$ in Eq. (35) and $B_{2\Delta N\Delta}$ in Eq. (37)), where neglected as they are negligible small.

We write now the RPA contribution to the response function as,

$$R_{PP}^{RPA} = \tilde{R}_1 + R_{12} + R_2, \quad (40)$$

where we have redefined $\tilde{R}_1 \equiv R_1 - R_{PP}^0$, R_{PP}^0 being the free response. This was done for convenience because the free response will be included within the self energy contribution.

Finally, if the residual interaction V , fulfills the three conditions quoted at the beginning of this sub section then R_2 accounts with good accuracy for the full direct plus exchange RPA. As we will show in the next section in general this is not the case. Then V should be split into two terms V_1 and V_2 , where the first is a contact interaction while V_2 is chosen in such a way that a fast convergence to the RPA series is achieved. In addition to the perturbative terms in V_2 , it appears two new terms R_1 and R_{12} . In this sub section we have presented a scheme to deal with them.

2.2 Self Energy insertions:

We consider now self energy insertions over a single ph or Δh bubble. This means to neglect V_{PP} in Eq. (8). That is,

$$G_{PP}(\hbar\omega) = \frac{1}{\hbar\omega - H_0 - \Sigma^{PQP} + i\eta} - \frac{1}{\hbar\omega + H_0 + \Sigma^{PQP} - i\eta}, \quad (41)$$

we insert Eq. (41) into Eq. (7) and using the definition of P , we write the response function which contains the Lindhard (L) plus self energy (SE) contributions as,

$$R_{PP}^{L+SE} = R_{NN}^{L_N+SE} + R_{N\Delta}^{SE} + R_{\Delta\Delta}^{L_\Delta+SE}, \quad (42)$$

where,

$$R_{NN}^{L_N+SE} = -\frac{1}{\pi} \text{Im} \sum_{ph, p'h'} \mathcal{O}_N^\dagger \langle ph | \frac{1}{\hbar\omega - H_0 - \Sigma^{P_N Q P_N} + i\eta} | p'h' \rangle \mathcal{O}_N, \quad (43)$$

$$R_{N\Delta}^{SE} = -\frac{1}{\pi} \text{Im} \sum_{ph, \Delta h} \mathcal{O}_N^\dagger \langle ph | \frac{1}{\hbar\omega - H_0 - \Sigma^{P_N Q P_\Delta} + i\eta} | \Delta h \rangle \mathcal{O}_\Delta, \quad (44)$$

$$R_{\Delta\Delta}^{L_\Delta+SE} = -\frac{1}{\pi} \text{Im} \sum_{\Delta h, \Delta' h'} \mathcal{O}_\Delta^\dagger \langle \Delta h | \frac{1}{\hbar\omega - H_0 - \Sigma^{P_\Delta Q P_\Delta} + i\eta} | \Delta' h' \rangle \mathcal{O}_\Delta \quad (45)$$

for simplicity only forward going contribution were shown. The notation L_N refers to the Lindhard function while L_Δ represents the Δh bubble.

Self energy insertions are not diagonal in P -space. We must consider diagonal and non diagonal self energy insertions, shown in Figs. 4 and 5, respectively. In these

figures only second order contributions are presented. Non diagonal contributions which connects P_N and P_Δ spaces with the self energy attached to the same fermionic line cancel due to the isospin summation. We analyzed now in detail diagonal self energy insertions. Regarding non diagonal terms, there are 16 different contributions to it when keeping terms up to second order. They will be evaluated in the next section and formal expressions are obtained from the standard rules for Goldstone diagrams. In Fig. 5 we show some of these diagrams.

Diagonal second order self energy contributions are divergent. To overcome this difficulty one possibility is to implement some renormalization procedure [10]. The other alternative is to sum self energy up to infinite order, as was done in previous works (see refs. [22] and [23]). We extend now the procedure developed in ref. [22] to include the $\Delta(1232)$.

From Eq. (9) diagonal matrix elements for the self energy can be draw as,

$$\begin{aligned} \langle P | \Sigma^{PQP} | P \rangle &= \sum_Q \langle P | V | Q \rangle_{D+E} \frac{1}{\hbar\omega - E_{QQ}^0 + i\eta} \langle Q | V | P \rangle_{D+E} - \\ &- \sum_Q \langle P | V | Q \rangle_{D+E} \frac{1}{\hbar\omega + E_{QQ}^0 - i\eta} \langle Q | V | P \rangle_{D+E}, \end{aligned} \quad (46)$$

where $|P\rangle$ can be either a ph or Δh configuration, $|Q\rangle$ is any of the Q -configurations and $H_0|Q\rangle = E_{QQ}^0|Q\rangle$.

In Fig. 6, we have isolated a graphical representation of the direct self energy Σ^{PQP} restricting ourselves to the Q -space. Notice that each contribution has a closed fermionic loop (a ph or Δh bubble) and two open fermionic lines, one of which is always a hole. Performing the summation over spin and isospin and making the conversion of sums over momenta to integrals it is easy to see that these matrix elements can be written as a function of the energy momentum of the external probe and the momentum of the hole line,

$$\langle P | \Sigma^{PQP} | P \rangle = \Sigma^{PQP}(\mathbf{h}, \mathbf{q}, \hbar\omega). \quad (47)$$

Through the numerical analysis it turns out that the dependence of the self energy over the hole momentum is not very strong. This allows us to make an average over it,

$$\Sigma^{PQP}(\mathbf{h}, \mathbf{q}, \hbar\omega) \xrightarrow{[average \ over \ \mathbf{h}]} \Sigma^{PQP}(\mathbf{q}, \hbar\omega). \quad (48)$$

as described in Appendix C. This approximation is not so good when the self energy is attached to a hole line, but this contribution is by itself very small. In Appendix C we also show explicit expressions for each self energy contributions. Let us call,

$$\Sigma^{NN}(\mathbf{Q}, \nu) = \sum_{i=1}^4 \Sigma^{P_N Q_i P_N}(\mathbf{Q}, \nu). \quad (49)$$

and

$$\Sigma^{\Delta\Delta}(\mathbf{Q}, \nu) = \sum_{i=1}^4 \Sigma^{P_\Delta Q_i P_\Delta}(\mathbf{Q}, \nu). \quad (50)$$

where the different Q_i , are defined in Fig. 6. We have used dimensionless quantities $\mathbf{Q} = \mathbf{q}/k_F$ and $\nu = \hbar\omega/2\varepsilon_F$; k_F and ε_F being the Fermi momentum and energy, respectively.

We defined now the functions $\Lambda(\mathbf{Q}, \nu)$ and $\Gamma(\mathbf{Q}, \nu)$ for the real and imaginary part of the self energy,

$$Re \Sigma^{NN(\Delta\Delta)}(\mathbf{Q}, \nu) \equiv \Lambda^{NN(\Delta\Delta)}(\mathbf{Q}, \nu) \quad (51)$$

and

$$Im \Sigma^{NN(\Delta\Delta)}(\mathbf{Q}, \nu) \equiv -\frac{1}{2} \Gamma^{NN(\Delta\Delta)}(\mathbf{Q}, \nu). \quad (52)$$

The diagonal contributions from Eq. (43) and Eq. (45) gives,

$$(R_{PP}^{L_P+SE})^{diag.} = -\frac{1}{\pi} Im \sum_P \langle \mathcal{O}^\dagger | P \rangle \frac{(2\varepsilon_F)^{-1}}{\nu - \varepsilon_P - \Lambda^{PP}(\mathbf{Q}, \nu) + i\Gamma^{PP}(\mathbf{Q}, \nu)/2} \times \langle P | \mathcal{O} \rangle. \quad (53)$$

where $H_0 |P\rangle = 2\varepsilon_F \varepsilon_P |P\rangle$. This expression can be rewrite as (see ref. [22] for details),

$$(R_{PP}^{L_P+SE})^{diag.} = \int_0^\infty dE R_{PP}^0(\mathbf{Q}, E) \frac{1}{2\pi} \frac{\Gamma^{PP}(\mathbf{Q}, \nu)}{(E - \nu + \Lambda^{PP}(\mathbf{Q}, \nu))^2 + (\Gamma^{PP}(\mathbf{Q}, \nu)/2)^2}. \quad (54)$$

where the free response is,

$$R_{PP}^0(\mathbf{Q}, E) = (2\varepsilon_F)^{-1} \sum_P |\langle P | \mathcal{O} \rangle|^2 \delta(\varepsilon_P - E), \quad (55)$$

Finally, two points deserve special attention. The first one refers to the exchange terms to the self energy. Diagonal exchange contributions are shown in Fig. 7 for Q_1 space and explicit expressions can be found in Appendix C. They were included just

for completeness but its contribution is very small. Non diagonal exchange contributions were analyzed in ref. [23] for the ph sector. In the next section we will see that direct non diagonal contributions are in itself small. For this reason, these exchange contributions were not considered at all.

As a second point we want to consider again Eq. (7). In the first subsection we have neglected the self energy and we have solved the problem of a general Hamiltonian leading to the RPA correlations. In the second subsection we have dressed ph and Δh -bubbles with self energy insertions. In ref. [22] we have used these dressed bubbles to re-calculate the ring series. We will not attempt to do this kind of calculations here due to the presence of exchange terms in the RPA series which will give rise to some exchange terms of third and higher order very difficult to evaluate. A scheme which accounts for these contributions is not available at present.

From both subsections, the response function is expressed as the sum of Eqs. (40) and (42), as

$$R_{PP} = R_{PP}^{RPA} + R_{PP}^{L+SE}. \quad (56)$$

In the next section we will analyze numerically these contributions.

3 Results and Discussion.

In this section we give numerical values and discuss the different terms coming from our scheme and in particular we analyze the influence of the $\Delta(1232)$. We will follow the notation and the ordering of the last section. At the end of this section we compare our results with data from the transverse response of ^{40}Ca . All calculations were done for nuclear matter with an effective Fermi momentum $k_F = 235 \text{ MeV}/c$ [13].

For the parameters entering into our theory we have set at 140 MeV (770 MeV) the mass of the pion (rho meson). The pion coupling constant $f_{\pi NN}^2/4\pi=0.081$, $f_{\pi\Delta N}=2$ $f_{\pi NN}$ and $f_{\pi\Delta\Delta}=\frac{4}{5}f_{\pi NN}$. For the rho meson we have used $C_{\rho NN} = C_{\rho\Delta N} = C_{\rho\Delta\Delta} = 2.18$. The different mesons cut-offs at the vertices are set to $\Lambda_{\pi NN} = 1300 \text{ MeV}/c$, $\Lambda_{\rho NN} = 1750 \text{ MeV}/c$ while all the remaining cut-offs are set to 1000 MeV/c. For the Landau Migdal parameters we have taken $g_{NN} = 0.3$ and $g'_{NN} = 0.7$, while different values for $g'_{\Delta N}$ and $g'_{\Delta\Delta}$ are considered.

As mentioned, we discuss now in two subsections the RPA correlations and the self energy insertions, respectively. At the end of the second subsection, we consider the RPA plus self energy results. All this is done for three energy regions: the quasi elastic peak, the $\Delta(1232)$ -peak and the 'dip' region (that is, the region in between the two previous ones). We name the first and second regions as the NN and $\Delta\Delta$ sectors.

It is more convenient to analyze the structure function rather than the response function which means to put the electromagnetic form factors equal to one ($G_E = G_\Delta = 1$). This allows a better understanding of the different contributions entering into our scheme. Even though, in the last section we have preferred to show the response function. As there are two different electromagnetic form factors, it could be confusing to construct the response function from the structure function. That is, some terms should be multiplied by G_E^2 , others by G_Δ^2 and finally others by $G_E G_\Delta$. In what follows, we analyzed then the structure function per unit volume except when we compare with data.

3.1 RPA results:

We start by analyzing the validity of the scheme presented in subsection 1.1. The transverse structure function per unit volume at momentum transfer $q = 410 \text{ MeV}/c$ is studied in detail. The first step is to build a contact plus finite range interaction which fulfills all the conditions required for V_2 . As the finite range piece of the interaction is fixed by the $(\pi + \rho)$ -meson exchange potential, the problem is reduced to find an appropriate set of Landau Migdal parameters (which represent the contact piece of the interaction). We define,

$$g'_{PP} = g'_{1PP} + g'_{2PP}, \quad (57)$$

where PP can be either NN , ΔN or $\Delta\Delta$. Obviously, g'_{1PP} (g'_{2PP}) is the Landau Migdal parameter associated with V_1 (V_2). The g'_{NN} parameter was already fixed at 0.7, the g_{NN} parameter is fixed at 0.3 and is completely assigned to V_1 . Different values for $g'_{\Delta N}$ and $g'_{\Delta\Delta}$ will be considered.

From the numerical calculations it turns out that the appropriate set of Landau Migdal parameters entering in V_2 , are the following $g'_{2NN} = 0.5$, $g'_{2\Delta N} = 0.0$ and

$g'_{2\Delta\Delta} = 0.3$. This interaction is called V_a in Table I. As a further simplification all form factors were evaluated at q . In Fig. 8, we compare direct first and second order in V_2 contributions with the full ring series (where the free structure function was subtracted). This is done also for V_b interaction. We see that the agreement is rather good for V_a while it is poor for V_b . In addition, the relative magnitude of the ring contribution with respect to the free structure function shows that the disagreement is unacceptable for V_b , specially within the Δ -region.

We have found then an interaction V_a , for which its two first direct perturbative terms account for the full ring series. Next step is to check that the exchange terms are smaller than the corresponding direct ones. Let us consider three different contributions, called B_{NN} , $B_{\Delta N}$ and $B_{\Delta\Delta}$, depending on the hadronic vertex where the external operator is attached. More explicitly, B_{1NN} ($B_{1\Delta\Delta}$) is the sum of the first and second (third and fourth) graphs on line R_2 of Fig. 2. Each subindex 1, indicates that those are first order contributions. Only V_{NN} contribute to B_{1NN} and similarly $V_{\Delta N}$ ($V_{\Delta\Delta}$) to $B_{1\Delta N}$ ($B_{1\Delta\Delta}$). In higher order terms to $B_{NN(\Delta N, \Delta\Delta)}$ all interactions V_{NN} , $V_{\Delta N}$ and $V_{\Delta\Delta}$ are present (this can be easily seen in Eq. (33)). Before going on, we must say that the $B_{\Delta N}$ contribution has very particular features which deserves special attention. For this reason we discuss now B_{NN} and $B_{\Delta\Delta}$ and then we go back to $B_{\Delta N}$.

In Table II, we show direct and exchange first order contributions B_{1NN} and $B_{1\Delta\Delta}$ to the RPA series ². We show results for the two interactions above mentioned V_a and V_b . First we note that for V_a it holds the condition that exchange terms keeps smaller than the corresponding direct ones. This is not the case in V_b for the $\Delta\Delta$ channel. At this point, we have to mention that we have used the notation *direct* and *exchange* following the standard notation for those graphs. When the Δ is involved, direct plus exchange contributions do not imply antisymmetrization as the Δ is a distinguishable particle from nucleons. At variance with the nucleon sector, exchange terms should be seen as a particular set of graphs which are present in the RPA series and eventually can be bigger than the corresponding direct ones. In fact, there is a compromise for the values of the parameters entering into the interaction between

²We have preferred to present only first order contributions. The extremes of the second order ones occurs at different energy values, which would increase the size of the table with no additional information.

the fast convergence of the perturbative terms to the ring series (shown in Fig. 8) and the condition over exchange terms.

Note that even the starting interaction is the same for both direct and exchange contributions, for the direct ones only the central piece of the interaction survives, while for the exchange contribution both the central and the tensor term contribute (see for instances, Eqs. (72) and (73) in Appendix B). In particular, this means that the pion contributes to the exchange terms only.

One of the aims of this work is to study the role played by exchange terms in the RPA. All second order exchange contributions are included and also some higher order ones. We recall that the residual interaction was split into a contact term (V_1), for which exchange terms can be sum up to infinite order and a finite range piece (V_2), for which exchange terms are considered up to second order. Also cross exchange terms between V_1 and V_2 are included up to second order in V_2 and infinite order in V_1 . In [17] we have discussed an alternative scheme, in which direct contributions are considered up to infinite order through the RA and exchange ones are added up to second order. In that work, we saw that this is not a good approximation for the NN sector. Also, from table II, it is observed that the situation is even worse for the $\Delta\Delta$ sector where for V_b exchange contributions are bigger than the corresponding direct ones.

We turn now to $B_{\Delta N}$ which is dominated by $V_{\Delta N}$. As mentioned in the last section, no contact term in the residual interaction which connects P_N and P_Δ spaces survives. That means that the direct contact contribution (proportional to $g'_{\Delta N}$) is exactly cancel by the corresponding exchange one. Then only the finite range piece of the interaction contribute. Note that the advantage of our method to evaluate exchange terms relays on the fact that exchange terms from contact interaction can be sum up to infinite order. But when contact terms exactly cancels, there is no way out but to evaluate each exchange term perturbatively. And in practice, we can evaluate them up to second order.

Fortunately, the particular behavior of $B_{\Delta N}$ allows a perturbative treatment up to second order. First, for V_a ($g'_{\Delta N} = 0$), the two first direct terms reproduce the RA almost exactly. Secondly, $B_{1\Delta N}$ has two extremes where each one coincides with the maximum of the free structure function for the nucleon and delta peaks. In Table III

we show first and second order contributions to $B_{\Delta N}$. One striking feature is that exchange terms are bigger than the corresponding direct ones. This is because of the tensor term of the interaction which contribute to the exchange term only. In column *exc (w.t.)* of the same table, we present exchange terms without the tensor contribution. In this case, exchange terms are smaller than the corresponding direct ones.

In Fig. 9 we present direct plus exchange contribution to $B_{\Delta N}$. In this figure and Table III, note that while direct contribution to $B_{\Delta N}$ is positive in the NN sector, the exchange terms makes the whole contribution to be negative. Also, in the figure we show the RA result for several values of $g'_{\Delta N}$. From Appendix A, we see that for g'_{NN} , g_{NN} and $g'_{\Delta\Delta}$ direct plus exchange contact terms can be account by a re-definition of these parameters. That means that if one wants to adjust $g'_{NN(\Delta\Delta)}$ and g_{NN} by reproducing any experimental process, one should take only direct matrix elements for them. But this is not the case for $g'_{\Delta N}$ where the exchange term exactly cancel the direct one. Surprisingly, the RA with a non zero $g'_{\Delta N}$ value reproduce reasonably well the behavior of the RPA with the V_a interaction in the NN sector. In the first case it is $g'_{\Delta N}$ which dominates, while in the second case it is the tensor force (not present in RA). It is widely accepted that these kind of correlations with the $\Delta(1232)$ reduce the intensity of the transverse quasi elastic structure function. Our result confirm this, but for a very different reason.

Going back to our scheme, from Table III we observe that exchange term are considerably reduced from first to second order in the NN sector. The situation is not so good in the $\Delta\Delta$ sector. Even thought, $B_{\Delta N}$ is small in comparison with the free structure function in the $\Delta\Delta$ sector.

Let us resume these considerations about the applicability of the scheme. We have found an interaction V_a for which its firsts two direct perturbative terms accounts for the whole RA and whose exchange terms are smaller than the corresponding direct ones for B_{NN} and $B_{\Delta\Delta}$. Even this does not hold for the exchange $B_{\Delta N}$ term, we will evaluate it up to second order as this term is small in comparison with the free structure function. Going back to Eq. (25) we see that V_2 (whose value is V_a for the present calculation), fix the finite range piece of the interaction. We can vary freely the contact V_1 interaction to construct V . As already mentioned, the only remaining

constraint is that V_1 should allow a perturbative treatment.

Now we consider final results for the nuclear structure function. In Fig. 10, we study the effect of the Δ over the nuclear structure function in the NN sector. We show both RPA results with and without the Δ . The Landau Migdal parameters are the ones named by V_b ($V_b = V_1 + V_a$) in Table I. Formally, $V_{\Delta\Delta}$ has an effect on this sector, but the numerical analysis shows that this is negligible small. It is $V_{\Delta N}$ which dominates the Δ contribution over this sector. As no $g'_{\Delta N}$ parameter appears, we show results for only one interaction. We see that the Δ reduce the RPA structure function in an appreciable way. To get a better understanding of the effect of RPA correlations over the structure function, we define the quantity,

$$\gamma(\mathbf{q}, \hbar\omega) = 100 \frac{R_{PP}^{RPA}(\mathbf{q}, \hbar\omega) - R_{PP}^0(\mathbf{q}, \hbar\omega)}{R_{PP}^0(\mathbf{q}, \hbar\omega)}, \quad (58)$$

which is displayed in Fig. 10 b. The Δ reduce the intensity of the quasi elastic peak. While RPA correlations without the Δ produce a redistribution of the intensity within the NN sector keeping the energy weight sum rule unchanged, $V_{\Delta N}$ translates intensity from the NN - to the $\Delta\Delta$ -sector (as already shown in Fig. 9). Obviously, the energy weight sum rule is also unchanged but within the full energy region.

In Fig. 11, we present the RPA structure function for several residual interaction for both the NN and $\Delta\Delta$ -sectors. We vary only $g'_{\Delta\Delta}$ from 0.4 to 0.6. Also, in Fig. 11 b, we show $\gamma(\mathbf{q}, \hbar\omega)$. The effect of RPA correlations is analogous in both sectors. Note that the changes in $V_{\Delta\Delta}$ makes no appreciable change in the NN -sector. Also, as $g'_{\Delta\Delta}$ grows, this more repulsive interaction moves the delta peak towards higher energies. Small changes on the $g'_{\Delta\Delta}$ value makes small changes in the RPA structure function.

In Fig. 12, we compare the RPA result with the RA one (that its, is corresponding direct terms). For RA, we have used $g'_{\Delta N} = 0.43$ induced by Fig. 9. From Fig. 12, we note first that also for direct terms, changes in $g'_{\Delta\Delta}$ produce no appreciable changes in the NN sector. But the striking point is the extreme sensibility of the RA result over the $g'_{\Delta\Delta}$ value in the $\Delta\Delta$ sector. At variance the RPA structure function has a smooth behavior. This is a consequence of exchange terms, which happens to be very important. This is already suggested by Eq. (66) for instance, where for a contact interaction the exchange term reduce the $g'_{\Delta\Delta}$ parameter in about 70 %.

Finally, note that the RA approximation with $g'_{\Delta N}$ and $g'_{\Delta\Delta}$ parameters gives a reasonable result only in the NN sector, although it is questionable how to fix $g'_{\Delta N}$.

3.2 Self Energy results:

We go on analyzing the structure function per unit volume at momentum transfer $q = 410$ MeV/c by including self energy insertions. In Fig. 13, we show the imaginary part of the self energy. Notice that the quantity we have called self energy is in fact part of a full set of diagrams and through an average procedure it depends upon the momentum and energy of the external probe. It is at variance with other calculations where self energy insertions depends on the variables of the particle (hole or Δ), where it is attached (see refs. [26, 28, 29]).

In Fig. 13 a), we have plotted $Im \Sigma^{P_N Q P_N}$ for V_c from Table I. The non vanishing values for $Im \Sigma^{P_N Q_4 P_N}$ lays outside the energy region of interest. From all self energy insertions $\Sigma^{P_N Q_1 P_N}$ is the most widely studied. Our result is in agreement with other calculations where an empirical optical potential is used (see ref. [19] for instance). Within a more complex scheme, analogous correlations are considered in the optical Green function approach [24]. Self energy for the Δ are presented in Fig. 13 b). We have a qualitative agreement with the existing values for $Im \Sigma^{P_\Delta Q_1 P_\Delta}$ from refs. [26] and [28], even a rigorous comparison is not possible due to the particularities of the average procedure we have mentioned. Also in Fig 13 a) and b), we present results for $Im \Sigma^{P_{N(\Delta)} Q_{2,3} P_{N(\Delta)}}$, which are shown for completeness. We concentrate now on $\Sigma^{P_{N(\Delta)} Q_1 P_{N(\Delta)}}$.

With respect to the exchange terms for both $\Sigma^{P_N Q_1 P_N}$ and $\Sigma^{P_\Delta Q_1 P_\Delta}$, they are shown in Table IV. At variance with RPA correlations, exchange contributions are small. In addition, due to the different kind of sums over spin and isospin, no cancellation occurs for $g'_{\Delta N}$.

In Fig. 14, we study the dependence of $Im \Sigma^{P_\Delta Q_1 P_\Delta}$ over some of the parameters entering in our scheme. In Fig. 14 a), we vary the contact Landau Migdal $g'_{\Delta N}$ parameter, keeping fixed all other parameters and constants. We see that $Im \Sigma^{P_\Delta Q_1 P_\Delta}$ is rather sensible to the $g'_{\Delta N}$ value. In Fig. 14 b), we analyzed different values for the meson-delta-nucleon cut offs, which are more uncertain than the corresponding meson-nucleon-nucleon ones. Without form factors, self energy insertions would be

divergent. Thus the election of the cut off is crucial in the evaluation of the self energy. At a first glance, curves b1-b3 may be seeing as contradictory, as the self energy grows for decreasing values of the cut off. This behavior is a consequence of having chosen $\Lambda_{\pi\Delta N} = \Lambda_{\rho\Delta N}$. In the analogous expression of Eqs. (15) and (16) for the ΔN channel we see that there is a competition of the ρ -meson and g' and the ρ -meson and the pion in \tilde{g}' and \tilde{h}' , respectively. Due to the different masses of the pion and the rho meson, a strong reduction on the rho meson interaction occurs as the cut off decrease while this reduction is less pronounce for the pion. That is, even all terms are reduced, the significant reduction of the rho meson makes the whole interaction stronger. Curve b4, where we have taken a different value for $\Lambda_{\pi\Delta N}$ and $\Lambda_{\rho\Delta N}$, shows an important reduction.

Before going on analyzing the structure function which results from diagonal self energy insertions, let us consider non diagonal contributions. Non diagonal self energy insertions where evaluate up to second order in the residual interaction V_c . There are 16 different graphs to it, two of which have no Δ . Some of them are plotted in Fig. 5. In Fig. 15 a), we present the contributions for all non diagonal self energy insertions to the structure function. These contributions produce a small redistribution of the intensity. No exchange term were considered. In ref. [23] we have showed that exchange terms are negligible small for the NN sector. In Fig. 15 b), we see that this contribution is not significant.

In Fig. 16, we show the results for the diagonal self energy insertion over the structure function. The general effect of self energy insertions is to produce a redistribution of the intensity from the low to the high energy region for both the NN and $\Delta\Delta$ sectors. The peaks are reduced in intensity and shifts to lower energies, while intensity appears in the dip region and also at energies beyond the $\Delta\Delta$ peak. In this figure we show results for both $\Sigma^{P_{N(\Delta)}Q_1P_{N(\Delta)}}$ and $\Sigma^{NN(\Delta\Delta)}$ (see eqs. (49) and (50)). Note that even $Im \Sigma^{P_\Delta Q_4 P_\Delta}$ is zero within the energy region of interest, the same do not holds for its real part. It is not easy to established which are the appropriate values for the self energies when the Δ is involved. As we have shown in Fig. 14, the self energy depends strongly on the interaction (and in particular on its cut offs for the mesons form factors). It means that within the uncertainty in the election of the interaction, strongly different results for the self energy can be obtained. The

aim of this work is to present the scheme and analyzed the general features of each contribution. For $\sum P_{N(\Delta)} Q_{2,3,4} P_{N(\Delta)}$ self energy insertions, a deeper analysis for different interactions is desirable. Due to this and due to the fact that only $\sum P_{N(\Delta)} Q_1 P_{N(\Delta)}$ exchange terms where evaluated, we prefer to take only the $\sum P_{N(\Delta)} Q_1 P_{N(\Delta)}$ self energy as our final result. The effect of the Δ over the NN quasi elastic peak is not significant at low energies. For increasing values of the energy it becomes more important producing an increase of the intensity, being very relevant in the dip region.

Finally, in Fig. 17 we compare our final result of Eq. (56) with data at momentum transfer $q = 410$ and 550 MeV/c. In this case, we have plotted the transverse response function for ^{40}Ca . It is not our intention to reproduce the data. But we wanted to include this figure in order to see how do the different contributions stemming from our scheme compares with the experimental points. We consider this result encouraging as the interaction chosen is very simple, in particular the set of cut offs and coupling constants when the Δ is involved. And also because other mechanisms, like ground state correlations beyond RPA ($2p - 2h$ states) and MEC add intensity in this region. Note the behavior around the dip, only the Δ can produce the change in the slope at high energies suggested by data. As mentioned, additional intensity is provided by $2p - 2h$ and MEC.

4 Conclusions

In this work we have addressed the role played by the $\Delta(1232)$ in the nuclear transverse response for quasi elastic electron scattering. This was done by including RPA correlations and self energy insertions. All calculations were done in nuclear matter.

We have presented a formalism which explicitly includes the Δ and exchange terms in the RPA series. At variance with direct terms which can be sum up to infinite order, exchange terms should be evaluated perturbatively. In our scheme we have divided the residual interaction in a weak finite range plus contact term and the remainder contact one. As for direct terms of any interaction, exchange terms for a contact interaction can also be sum up to infinite order. These allows the inclusion of higher order exchange terms.

The effect of exchange terms is important in both the nucleon and the Δ peak

sectors. In the Δ sector the RA gives a narrow peak not suggested by the double differential cross section for (e, e') . The addition of exchange terms produce a curve which shape is analogous to the one in the nucleon sector. Also the role of interference terms between the nucleon and the Δ sectors was clarified. Exchange terms cancel the contact $g'_{\Delta N}$ Landau Migdal parameter. The result for these interference terms is governed by the tensor piece of the $V_{\Delta N}$ interaction, given a redistribution of the intensity from the nuclear to the Δ sector.

The final result for RPA correlations is to redistribute the intensity from the low to the high energy region, keeping the energy weight sum rule unchanged. The direction towards the intensity moves is a consequence of the repulsive character of the interaction.

We have considered self energy insertions which dressed a single ph and Δh bubble. They were divided into two sets, depending on which bubble they act and then, subdivided into four terms depending on the intermediate states (see eqs. (49) and (50)). Sums over spin and isospin are very different from the RPA ones and so the integration over the internal momentum. For direct self energy insertions the tensor term of the interaction is present, no cancellation of $g'_{\Delta N}$ occurs and exchange terms are unimportant.

Self energy insertions produce also a redistribution of the intensity from the low to the high energy regions. But while RPA correlations makes this redistribution within ph and Δh states, the self energy opens new channels like $2p - 2h$ and higher order states. This is specially important for the dip region, even a complete description should include ground state correlations beyond RPA and MEC. Finally, self energy insertions are very sensitive to the residual interaction employed.

As a final remark, let us mentioned that we have preferred not to compare our result with the double differential cross section for (e, e') . The reason for this is twofold. First, the longitudinal response function should be included and discussed. In this sense, the residual interaction should be modified. Secondly, this double differential cross section could be a tool to study deeper the residual interaction for the Δ , which is beyond the scope of the present work.

Acknowledgments

I would like to thank O. Civitarese for fruitful discussions and for the critical reading of the manuscript. Also I would like to thank C. F. Williamson for communicating the ^{40}Ca experimental points of the MIT-Bard College-Louisiana State University-Northwestern University-Ohio University collaboration. This work has been partially supported by the Agencia Nacional de Promoción Científica y Tecnológica, under contract PMT-PICT-0079.

APPENDIX A

In this appendix we show how to modified Landau Migdal parameters to account for exchange term. The direct V_1 interaction for each P -channel needed in the RPA, are,

$$V_{1\,NN} = \frac{f_{\pi NN}^2}{\mu_\pi^2} (g_{1\,NN} \boldsymbol{\sigma} \cdot \boldsymbol{\sigma}' + g'_{1\,NN} \boldsymbol{\tau} \cdot \boldsymbol{\tau}' \boldsymbol{\sigma} \cdot \boldsymbol{\sigma}'), \quad (59)$$

$$V_{1\,\Delta N} = \frac{f_{\pi NN} f_{\pi \Delta N}}{\mu_\pi^2} g'_{1\,\Delta N} \boldsymbol{\tau} \cdot \mathbf{T}' \boldsymbol{\sigma} \cdot \mathbf{S}', \quad (60)$$

$$V_{1\,\Delta\Delta} = \frac{f_{\pi \Delta N}^2}{\mu_\pi^2} g'_{1\,\Delta\Delta} \boldsymbol{\tau} \cdot \mathbf{T}' \boldsymbol{\sigma} \cdot \mathbf{S}'. \quad (61)$$

There is two ways to obtained the exchange terms. One is to act with exchange operators P_σ and P_τ over the direct interaction (see for instance the appendix of ref. [16]), then,

$$(V_{1\,NN})_E = -P_\sigma P_\tau V_{1\,NN}, \quad (62)$$

given the following values for the Landau Migdal parameters,

$$(g_{1\,NN})_E = \frac{1}{4} (g_{1\,NN} + 3g'_{1\,NN}), \quad (63)$$

$$(g'_{1\,NN})_E = \frac{1}{4} (g_{1\,NN} - g'_{1\,NN}). \quad (64)$$

Finally, the values needed to evaluate R_1 are, $(g_{1\,NN})_{D+E} = g_{1\,NN} + (g_{1\,NN})_E$ and $(g'_{1\,NN})_{D+E} = g'_{1\,NN} + (g'_{1\,NN})_E$.

We describe now an alternative and fully equivalent method [33]. Let us consider the $V_{1\,\Delta\Delta}$. We evaluate graph D and E of Fig. 18 using $V_{1\,\Delta\Delta}$. To evaluate $(g'_{1\,\Delta\Delta})_{D+E}$ one has to put matrices \mathbf{T} and \mathbf{S} in the external vertices to make sums over spin and isospin, respectively. Note that the mesonic vertices are different between D and E . After performing sums over spin and isospin we get,

$$(g'_{1\,\Delta\Delta})_{D+E} = \{g'_{1\,\Delta\Delta} - \frac{225}{64} \frac{f_{\pi NN} f_{\pi \Delta\Delta}}{f_{\pi \Delta N}^2} g'_{1\,\Delta\Delta}\}. \quad (65)$$

If we use, $f_{\pi \Delta N} = 2f_{\pi NN}$ and $f_{\pi \Delta\Delta} = \frac{4}{5}f_{\pi NN}$ we obtain,

$$(g'_{1\,\Delta\Delta})_{D+E} = \frac{19}{64} g'_{1\,\Delta\Delta}. \quad (66)$$

In an analogous way, it can be seen that $(g'_{1\,\Delta N})_{D+E} = 0$; a result already known [35].

APPENDIX B

In this Appendix, we present explicit expressions for the different graphs needed to build up our antisymmetric RPA for nuclear matter. We do not reproduce here the ph contributions as they were already published [17].

First, we need to define the Δ propagator,

$$G_\Delta(p) = \frac{1}{p_0 - \frac{\mathbf{p}}{2m_\Delta} - \delta m + i\eta} \quad (67)$$

where m_Δ is the $\Delta(1232)$ mass and δm is the mass difference between Δ and nucleon.

It is convenient to define now two function x and z related with the ph and Δh bubble, as,

$$x(\mathbf{Q}, \nu) = \int d^3h \frac{\theta(|\mathbf{h} + \mathbf{Q}| - 1)\theta(1 - h)}{\nu - (Q^2/2 + \mathbf{h} \cdot \mathbf{Q}) + i\eta} - \int d^3h \frac{\theta(|\mathbf{h} + \mathbf{Q}| - 1)\theta(1 - h)}{\nu + (Q^2/2 - \mathbf{h} \cdot \mathbf{Q})} \quad (68)$$

and

$$z(\mathbf{Q}, \nu) = \int d^3h \frac{\theta(1 - h)}{\nu - (\frac{c-1}{2}h^2 + c \mathbf{h} \cdot \mathbf{Q}) + \delta + i\eta} - \int d^3h \frac{\theta(1 - h)}{\nu + (\frac{c-1}{2}h^2 - c \mathbf{h} \cdot \mathbf{Q}) + \delta} \quad (69)$$

where $c = m/m_\Delta$ and $\delta = \delta m/(2\varepsilon_F)$. We have used dimensionless quantities as described in the text.

We show now first order contributions in V_2 . The external probe can create (or destroyed) a ph or Δh pair. The interference terms between these two pairs are,

$$(B_{1\Delta N}(\mathbf{Q}, \nu))_D = \frac{8}{3} \frac{1}{(2\pi)^3} \frac{A}{\hbar c \mu_\pi^2 k_F} \left(\frac{f_{\pi NN} f_{\pi \Delta N}}{4\pi \hbar c} \right) Q^2 \mu_v \mu_\Delta G_E G_\Delta \Gamma_{\pi NN}(Q) \Gamma_{\pi \Delta N}(Q) \tilde{g}'_{2\Delta N}(Q) x(\mathbf{Q}, \nu) z(\mathbf{Q}, \nu) \quad (70)$$

and

$$(B_{1\Delta N}(\mathbf{Q}, \nu))_E = -\frac{1}{6} \frac{1}{(2\pi)^3} \frac{A}{\hbar c \mu_\pi^2 k_F} \left(\frac{f_{\pi NN} f_{\pi \Delta N}}{4\pi \hbar c} \right) Q^2 \mu_\Delta \mu_v G_E G_\Delta \int d^3h \int d^3k \theta(1 - h) \theta(1 - |\mathbf{h} + \mathbf{k}|) \theta(|\mathbf{h} + \mathbf{Q} + \mathbf{k}| - 1) \Gamma_{\pi NN}(k) \Gamma_{\pi \Delta N}(k) \{8\tilde{g}'_{2\Delta N} + \tilde{h}'_{\Delta N} (3 - (\hat{\mathbf{k}} \cdot \hat{\mathbf{Q}})^2)\} \left\{ \frac{1}{\nu - \alpha_1 + i\eta} - \frac{1}{\nu + \alpha_1} \right\} \left\{ \frac{1}{\nu - \alpha_2 + i\eta} - \frac{1}{\nu + \alpha_2} \right\} \quad (71)$$

Expressions for the graphs shown in the third and fourth places of line R_2 of Fig. 2, are,

$$(B_{1\Delta\Delta}(\mathbf{Q},\nu))_D = \frac{32}{27(2\pi)^3} \frac{1}{\hbar c \mu_\pi^2 k_F} \left(\frac{f_{\pi NN} f_{\pi\Delta N}}{4\pi\hbar c} \right) Q^2 \mu_\Delta^2 G_E G_\Delta \Gamma_{\pi NN}(Q) \Gamma_{\pi\Delta N}(Q) \tilde{g}'_{2\Delta N}(Q) (z(\mathbf{Q},\nu))^2 \quad (72)$$

and

$$(B_{1\Delta\Delta}(\mathbf{Q},\nu))_E = -\frac{5}{3} \frac{1}{(2\pi)^3} \frac{A}{\hbar c \mu_\pi^2 k_F} \left(\frac{f_{\pi NN} f_{\pi\Delta\Delta}}{4\pi\hbar c} \right) Q^2 \mu_\Delta^2 (G_\Delta)^2 \int d^3h \int d^3k \theta(1-h) \theta(1-|\mathbf{h}+\mathbf{k}|) \Gamma_{\pi\Delta N}(k) \{10\tilde{g}'_{2\Delta\Delta} + \tilde{h}'_{\Delta\Delta} (3 + (\hat{\mathbf{k}} \cdot \hat{\mathbf{Q}})^2)\} \left\{ \frac{1}{\nu - \alpha_3 + i\eta} - \frac{1}{\nu + \alpha_3} \right\} \left\{ \frac{1}{\nu - \alpha_4 + i\eta} - \frac{1}{\nu + \alpha_4} \right\} \quad (73)$$

where we have defined,

$$\tilde{g}'_{2\Delta N}(k) = g'_{2\Delta N} - \frac{\Gamma_{\rho\Delta N}^2(k)}{\Gamma_{\pi\Delta N}^2(k)} C_{\rho\Delta N} \frac{k^2}{k^2 + \mu_\rho^2} \quad (74)$$

with an analogous expression for $\tilde{g}'_{2\Delta\Delta}$ and

$$\begin{aligned} \alpha_1 &= \frac{c-1}{2} h^2 + \frac{c}{2} Q^2 + c \mathbf{h} \cdot \mathbf{Q} + \delta, \\ \alpha_2 &= Q^2/2 + \mathbf{k} \cdot \mathbf{Q} + \mathbf{h} \cdot \mathbf{Q} \\ \alpha_3 &= \alpha_1 \\ \alpha_4 &= \frac{c-1}{2} h^2 + \frac{c-1}{2} k^2 + \frac{c}{2} Q^2 + (c-1) \mathbf{h} \cdot \mathbf{k} + c \mathbf{h} \cdot \mathbf{Q} + c \mathbf{k} \cdot \mathbf{Q} + \delta. \end{aligned} \quad (75)$$

Finally, $B_{1\Delta N} = (B_{1\Delta N})_D + (B_{1\Delta N})_E$ and $B_{1\Delta\Delta} = (B_{1\Delta\Delta})_D + (B_{1\Delta\Delta})_E$.

For second order contributions, we show exchange contributions only. It is straightforward to obtain direct ones. We need to present the expression for graphs B_{1NN} ,

$$(B_{1NN}(\mathbf{Q},\nu))_E = -\frac{1}{8} \frac{1}{(2\pi)^3} \frac{A}{\hbar c \mu_\pi^2 k_F} \left(\frac{f_{\pi NN}^2}{4\pi\hbar c} \right) Q^2 (\mu_\nu^2 - 3\mu_s^2) (G_E)^2 \int d^3h \int d^3k \theta(1-h) \theta(|\mathbf{p} + \mathbf{Q}| - 1) \theta(1-|\mathbf{h} + \mathbf{k}|) \theta(|\mathbf{h} + \mathbf{Q} + \mathbf{k}| - 1)$$

$$\begin{aligned}
& \Gamma_{\pi NN}^2(k) \{ \tilde{g}'_{2NN} + \tilde{h}'_{NN} ((\hat{\mathbf{k}} \cdot \hat{\mathbf{Q}})^2) \} \\
& \{ \frac{1}{\nu - \alpha + i\eta} - \frac{1}{\nu + \alpha} \} \{ \frac{1}{\nu - \alpha' + i\eta} - \frac{1}{\nu + \alpha'} \} \\
& \quad (76)
\end{aligned}$$

with

$$\begin{aligned}
\alpha &= Q^2/2 + \mathbf{h} \cdot \mathbf{Q} \\
\alpha' &= Q^2/2 + \mathbf{k} \cdot \mathbf{Q} + \mathbf{h} \cdot \mathbf{Q}
\end{aligned} \quad (77)$$

Also, we define the functions,

$$\begin{aligned}
\eta_{NN}(Q) &= \frac{m}{(2\pi)^2} \left(\frac{f_{\pi NN}^2}{4\pi\hbar c} \right) \frac{\tilde{g}'_{2NN}(Q)}{\hbar c \mu_\pi^2 k_F} \\
\eta_{\Delta N}(Q) &= \frac{m}{(2\pi)^2} \left(\frac{f_{\pi NN} f_{\pi \Delta N}}{4\pi\hbar c} \right) \frac{\tilde{g}'_{2\Delta N}(Q)}{\hbar c \mu_\pi^2 k_F} \\
\eta_{\Delta\Delta}(Q) &= \frac{m}{(2\pi)^2} \left(\frac{f_{\pi \Delta N}^2}{4\pi\hbar c} \right) \frac{\tilde{g}'_{2\Delta\Delta}(Q)}{\hbar c \mu_\pi^2 k_F}
\end{aligned} \quad (78)$$

Now second order exchange contributions are given by,

$$\begin{aligned}
B_{2NNN} &= 8 \eta_{NN} B_{1NN} x(\mathbf{Q}, \nu), \\
B_{2NN\Delta} &= \frac{64}{9} \eta_{N\Delta} B_{1NN} z(\mathbf{Q}, \nu), \\
B_{2N\Delta N} &= 8 \eta_{N\Delta} B_{1\Delta N} x(\mathbf{Q}, \nu), \\
B_{2\Delta NN} &= 8 \eta_{N\Delta} B_{1\Delta N} x(\mathbf{Q}, \nu), \\
B_{2N\Delta\Delta} &= \frac{64}{9} \eta_{\Delta\Delta} B_{1\Delta N} z(\mathbf{Q}, \nu), \\
B_{2\Delta N\Delta} &= \frac{64}{9} \eta_{\Delta N} B_{1\Delta N} z(\mathbf{Q}, \nu), \\
B_{2\Delta\Delta N} &= 8 \eta_{\Delta N} B_{1\Delta\Delta} x(\mathbf{Q}, \nu), \\
B_{2\Delta\Delta\Delta} &= \frac{64}{9} \eta_{\Delta\Delta} B_{1\Delta\Delta} z(\mathbf{Q}, \nu),
\end{aligned} \quad (79)$$

APPENDIX C

In this appendix we show explicit expressions for the self-energy insertions. Even direct contributions in the ph sector can be found in [22] and exchange ones are presented in [23], we reproduce them for completeness.

In Eqs. (49) we have,

$$\begin{aligned} \Sigma^{P_N Q_1 P_N}(\mathbf{h}, \mathbf{Q}, \nu) &= \frac{3}{2\pi^4} \left(\frac{f_{\pi NN}^2}{4\pi\hbar c} \right)^2 \frac{mc^2 k_F^4}{\mu_\pi^4} \int d^3 l \int d^3 p \Gamma_{\pi NN}^4(l) \theta(|\mathbf{p} + \mathbf{l}/2| - 1) \\ &\quad \theta(1 - |\mathbf{p} - \mathbf{l}/2|) (g_{NN}^2 + 3(\tilde{g}'_{NN})^2 + (\tilde{h}'_{NN})^2 + 2\tilde{g}'_{NN}\tilde{h}'_{NN}) \\ &\quad \{ \theta(|\mathbf{h} + \mathbf{Q} - \mathbf{l}| - 1) \frac{1}{\nu - \alpha_1 + i\eta} + \\ &\quad + \theta(1 - |\mathbf{h} + \mathbf{l}|) \frac{1}{\nu - \alpha'_1 + i\eta} \}, \end{aligned} \quad (80)$$

$$\begin{aligned} \Sigma^{P_N Q_2 P_N}(\mathbf{h}, \mathbf{q}, \nu) &= \frac{2}{3} \frac{mc^2 k_F^4}{\mu_\pi^4 \pi^4} \left(\frac{f_{\pi NN} f_{\pi \Delta N}}{4\pi\hbar c} \right)^2 \int d^3 k \int d^3 h' \theta(1 - h') \\ &\quad \Gamma_{\pi NN}^2(k) \Gamma_{\pi \Delta N}^2(k) (3(\tilde{g}'_{\Delta N})^2 + (\tilde{h}'_{\Delta N})^2 + 2\tilde{g}'_{\Delta N}\tilde{h}'_{\Delta N}) \\ &\quad \{ \theta(|\mathbf{h} + \mathbf{Q} - \mathbf{k}| - 1) \frac{1}{\nu - \alpha_2 + i\eta} + \\ &\quad \theta(1 - |\mathbf{h} + \mathbf{k}|) \frac{1}{\nu - \alpha'_2 + i\eta} \}, \end{aligned} \quad (81)$$

$$\begin{aligned} \Sigma^{P_N Q_3 P_N}(\mathbf{h}, \mathbf{q}, \nu) &= \frac{2}{3} \frac{mc^2 k_F^4}{\mu_\pi^4 \pi^4} \left(\frac{f_{\pi NN} f_{\pi \Delta N}}{4\pi\hbar c} \right)^2 \int d^3 k \int d^3 h' \theta(1 - h') \\ &\quad \theta(|\mathbf{h}' + \mathbf{k}| - 1) \Gamma_{\pi NN}^2(k) \Gamma_{\pi \Delta N}^2(k) \\ &\quad (3(\tilde{g}'_{\Delta N})^2 + (\tilde{h}'_{\Delta N})^2 + 2\tilde{g}'_{\Delta N}\tilde{h}'_{\Delta N}) \frac{1}{\nu - \alpha_3 + i\eta}, \end{aligned} \quad (82)$$

$$\begin{aligned} \Sigma^{P_N Q_4 P_N}(\mathbf{h}, \mathbf{q}, \nu) &= \frac{8}{27} \frac{mc^2 k_F^4}{\mu_\pi^4 \pi^4} \left(\frac{f_{\pi \Delta \Delta}^2}{4\pi\hbar c} \right)^2 \int d^3 k \int d^3 h' \theta(1 - h') \\ &\quad \Gamma_{\pi \Delta N}^4(k) (3(\tilde{g}'_{\Delta \Delta})^2 + (\tilde{h}'_{\Delta N})^2 + 2\tilde{g}'_{\Delta \Delta}\tilde{h}'_{\Delta N}) \frac{1}{\nu - \alpha_4 + i\eta} \end{aligned} \quad (83)$$

and Eqs. (50),

$$\begin{aligned}
\Sigma^{P_\Delta Q_1 P_\Delta}(\mathbf{h}, \mathbf{Q}, \nu) &= \frac{2}{3\pi^4} \left(\frac{f_{\pi NN} f_{\pi \Delta N}}{4\pi \hbar c} \right)^2 \frac{mc^2 k_F^4}{\mu_\pi^4} \int d^3 l \int d^3 p \Gamma_{\pi NN}^2(l) \Gamma_{\pi \Delta N}^2(l) \\
&\quad \theta(|\mathbf{p} + \mathbf{l}/2| - 1) \theta(1 - |\mathbf{p} - \mathbf{l}/2|) \theta(|\mathbf{h} + \mathbf{Q} - \mathbf{l}| - 1) \\
&\quad (3(\tilde{g}'_{N\Delta})^2 + (\tilde{h}'_{N\Delta})^2 + 2\tilde{g}'_{N\Delta}\tilde{h}'_{N\Delta}) \frac{1}{\nu - \alpha_1 + i\eta}, \tag{84}
\end{aligned}$$

$$\begin{aligned}
\Sigma^{P_\Delta Q_2 P_\Delta}(\mathbf{h}, \mathbf{q}, \nu) &= \frac{8}{27} \frac{mc^2 k_F^4}{\mu_\pi^4 \pi^4} \left(\frac{f_{\pi \Delta N}^2}{4\pi \hbar c} \right)^2 \int d^3 k \int d^3 h' \theta(1 - h') \\
&\quad \Gamma_{\pi \Delta N}^4(k) (3(\tilde{g}'_{\Delta\Delta})^2 + (\tilde{h}'_{\Delta\Delta})^2 + 2\tilde{g}'_{\Delta\Delta}\tilde{h}'_{\Delta\Delta}) \\
&\quad \theta(|\mathbf{h} + \mathbf{Q} - \mathbf{k}| - 1) \frac{1}{\nu - \alpha_2 + i\eta}, \tag{85}
\end{aligned}$$

$$\begin{aligned}
\Sigma^{P_\Delta Q_3 P_\Delta}(\mathbf{h}, \mathbf{q}, \nu) &= \frac{2}{3} \frac{mc^2 k_F^4}{\mu_\pi^4 \pi^4} \left(\frac{f_{\pi NN} f_{\pi \Delta\Delta}}{4\pi \hbar c} \right)^2 \int d^3 k \int d^3 h' \theta(1 - h') \\
&\quad \theta(|\mathbf{h}' + \mathbf{k}| - 1) \Gamma_{\pi NN}^2(k) \Gamma_{\pi \Delta\Delta}^2(k) \\
&\quad (3(\tilde{g}'_{\Delta N})^2 + (\tilde{h}'_{\Delta N})^2 + 2\tilde{g}'_{\Delta N}\tilde{h}'_{\Delta N}) \frac{1}{\nu - \alpha_3 + i\eta}, \tag{86}
\end{aligned}$$

$$\begin{aligned}
\Sigma^{P_\Delta Q_4 P_\Delta}(\mathbf{h}, \mathbf{q}, \nu) &= \frac{8}{27} \frac{mc^2 k_F^4}{\mu_\pi^4 \pi^4} \left(\frac{f_{\pi \Delta\Delta} f_{\pi \Delta N}}{4\pi \hbar c} \right)^2 \int d^3 k \int d^3 h' \theta(1 - h') \Gamma_{\pi \Delta\Delta}^2(k) \\
&\quad \Gamma_{\pi \Delta N}^2(k) (3(\tilde{g}'_{\Delta\Delta})^2 + (\tilde{h}'_{\Delta N})^2 + 2\tilde{g}'_{\Delta\Delta}\tilde{h}'_{\Delta N}) \frac{1}{\nu - \alpha_4 + i\eta} \tag{87}
\end{aligned}$$

where,

$$\begin{aligned}
\alpha_1 &= Q^2/2 + \mathbf{h} \cdot \mathbf{Q} - \mathbf{l} \cdot (\mathbf{h} + \mathbf{Q} - \mathbf{l})/2 + \mathbf{p} \cdot \mathbf{l} \\
\alpha'_1 &= Q^2/2 - l^2/2 + \mathbf{h} \cdot (\mathbf{l} - \mathbf{Q}) + \mathbf{p} \cdot \mathbf{l} \\
\alpha_2 &= Q^2/2 + \frac{c+1}{2} k^2 + \frac{c-1}{2} h'^2 + \mathbf{h} \cdot \mathbf{Q} - \mathbf{k} \cdot \mathbf{Q} - \mathbf{h} \cdot \mathbf{k} + c \mathbf{k} \cdot \mathbf{h}' + \delta \\
\alpha'_2 &= Q^2/2 + \frac{c+1}{2} k^2 + \frac{c-1}{2} h'^2 + \mathbf{h} \cdot \mathbf{Q} - \mathbf{k} \cdot \mathbf{h} + c \mathbf{k} \cdot \mathbf{h}' + \delta
\end{aligned}$$

$$\begin{aligned}
\alpha_3 &= \frac{c}{2}Q^2 + \frac{c+1}{2}k^2 + \frac{c-1}{2}h^2 + c\mathbf{h}\cdot\mathbf{Q} - c\mathbf{k}\cdot\mathbf{Q} - c\mathbf{h}\cdot\mathbf{k} + \mathbf{k}\cdot\mathbf{h}' + \delta \\
\alpha_4 &= \frac{c}{2}Q^2 + c k^2 + \frac{c-1}{2}h^2 + \frac{c-1}{2}h'^2 + c\mathbf{h}\cdot\mathbf{Q} + c\mathbf{k}\cdot\mathbf{h}' - c\mathbf{h}\cdot\mathbf{k} - c\mathbf{k}\cdot\mathbf{Q} + 2\delta
\end{aligned}$$

Exchange terms are given by,

$$\begin{aligned}
\Sigma^{P_N Q_{E1} P_N}(\mathbf{h}, \mathbf{q}, \nu) &= -\frac{1}{(2\pi)^4} \left(\frac{f_{\pi NN}^2}{4\pi\hbar c} \right)^2 \frac{mc^2 k_F^4}{\mu_\pi^4} \int d^3k \int d^3k' \\
&\quad \Gamma_{\pi NN}^2(k) \Gamma_{\pi NN}^2(k') \theta(1 - |\mathbf{h} + \mathbf{Q} - \mathbf{k} - \mathbf{k}'|) \\
&\quad \theta(|\mathbf{h} + \mathbf{Q} - \mathbf{k}| - 1) \theta(|\mathbf{h} + \mathbf{Q} - \mathbf{k}'| - 1) \\
&\quad (3\tilde{g}'^2 - (2(\hat{\mathbf{k}}\cdot\hat{\mathbf{k}'})^2 - 1)\tilde{h}'^2 + 2\tilde{g}'\tilde{h}') \frac{1}{\nu - \alpha_{E1} + i\eta} \quad (88) \\
\Sigma^{P_\Delta Q_{E1} P_\Delta}(\mathbf{h}, \mathbf{q}, \nu) &= -\frac{1}{6} \frac{mc^2 k_F^4}{\mu_\pi^4 \pi^4} \left(\frac{f_{\pi NN} f_{\pi \Delta N}}{4\pi\hbar c} \right)^2 \int d^3k \int d^3k' \theta(|\mathbf{Q} + \mathbf{h} - \mathbf{k}| - 1) \\
&\quad \theta(|\mathbf{Q} + \mathbf{h} - \mathbf{k}'| - 1) \theta(1 - |\mathbf{Q} + \mathbf{h} - \mathbf{k}' - \mathbf{k}'|) \\
&\quad \Gamma_{\pi NN}(k) \Gamma_{\pi NN}(k') \Gamma_{\pi \Delta N}(k) \Gamma_{\pi \Delta N}(k') \\
&\quad \{3\tilde{g}'_{\Delta N}(k)\tilde{g}'_{\Delta N}(k') + \frac{3}{2}\tilde{g}'_{\Delta N}(k)\tilde{h}'_{\Delta N}(k')(5 - 3(\hat{\mathbf{k}'}\cdot\hat{\mathbf{Q}})^2) + \\
&\quad \frac{3}{2}\tilde{g}'_{\Delta N}(k')\tilde{h}'_{\Delta N}(k)(5 - 3(\hat{\mathbf{k}}\cdot\hat{\mathbf{Q}})^2) + \\
&\quad \frac{1}{8}\tilde{h}'_{\Delta N}(k)\tilde{h}'_{\Delta N}(k') (2 + 3(\hat{\mathbf{k}}\cdot\hat{\mathbf{h}})^2 + 2\hat{\mathbf{Q}}\cdot(\hat{\mathbf{k}} \times \hat{\mathbf{k}}')^2 \\
&\quad - (\hat{\mathbf{Q}}\cdot\hat{\mathbf{k}})^2 - (\hat{\mathbf{Q}}\cdot\hat{\mathbf{k}'})^2 - (\hat{\mathbf{Q}}\cdot\hat{\mathbf{k}})(\hat{\mathbf{Q}}\cdot\hat{\mathbf{k}'})(\hat{\mathbf{k}}\cdot\hat{\mathbf{k}'}))\} \frac{1}{\nu - \alpha_{E2} + i\eta} \quad (89) \\
&\quad \quad \quad (90)
\end{aligned}$$

where,

$$\begin{aligned}
\alpha_{E1} &= Q^2/2 + \frac{c-1}{2}h^2 + \frac{c-1}{2}k^2 + \frac{c-1}{2}h'^2 - \\
&\quad (c-1)\mathbf{h}\cdot\mathbf{k} + (c-1)\mathbf{h}\cdot\mathbf{k}' + c\mathbf{k}\cdot\mathbf{k}' + \mathbf{h}\cdot\mathbf{q} + \delta
\end{aligned}$$

In order to simplify the calculation, it is a good approximation to eliminate the dependence on the hole momentum, by an average procedure (see ref. [22]), as follows,

$$\Sigma^{PQP}(\mathbf{Q}, \nu) \equiv \frac{1}{\frac{4}{3}\pi} \int d^3h \Sigma^{PQP}(\mathbf{Q}, \nu, \mathbf{h}) \quad (91)$$

References

- [1] P. Barreau *et al.*, Nucl. Phys. **A402** (1983) 515.
- [2] Z. E. Meziani *et al.*, Phys. Rev. Lett. **52** (1984) 2130.
- [3] Z. E. Meziani *et al.*, Phys. Rev. Lett. **55** (1985) 1233.
- [4] C. C. Blatchley, J. J. LeRose, O. E. Puet, D. Zimmermann, C. F. Williamsom and M. Deady, Phys. Rev. **C34** (1986) 1243.
- [5] J. Jourdan, Phys. Lett. **353B** (1995) 189; Nucl. Phys. **A603** (1996) 117.
- [6] J. V. Noble, Phys. Rev. Lett. **46** (1981) 412; Phys. Rev. **C27** (1983) 423. G. Do Dang and Nguyen van Giai, Phys. Rev. **C30** (1984) 731. H. Kurasawa and T. Suzuki, Nucl. Phys. **A454** (1986) 527. E. N. Nikolov, M. Bergmann, Chr. V. Christov, K. Goeke, A. N. Antonov and S. Krewald, Phys. Lett. **281B** (1992) 208.
- [7] R. J. Furnstahl and C. E. Price, Phys. Rev. **C40** (1989) 1398 C. J. Horowitz and J. Piekarewicz, Nucl. Phys. **A511** (1990) 461.
- [8] S. Fantoni and V. R. Pandharipande, Nucl. Phys. **A427** (1984) 473; A. Fabrocini and S. Fantoni, Nucl. Phys. **A503** (1989) 375; O. Benhar, A. Fabrocini and S. Fantoni, Nucl. Phys. **A550** (1992) 201.
- [9] W. M. Alberico, M. Ericson and A. Molinari, Ann. Phys. **154** (1984) 356.
- [10] W. M. Alberico, A. De Pace, A. Drago and A. Molinari, Rivista del Nuovo Cimento **14** (1991) 1.
- [11] J. W. van Order and T. W. Donnelly, Ann. Phys. **131** (1981) 451.
- [12] J. E. Amaro, A. M. Lallena, Nucl. Phys. **A537** (1992) 585; J. E. Amaro, G. Co', A. M. Lallena, Ann. Phys. **221** (1993) 306; J. E. Amaro, A. M. Lallena and G. CÓ, Nucl. Phys. **A578** (1994) 365.
- [13] J. E. Amaro, A. M. Lallena and G. CÓ, Int. J. Mod. Phys. **E3** (1994) 735.

- [14] F. A. Brieva and A. Dellafoore, Phys. Rev. **C36** (1987) 899.
- [15] C. García Recio, J. Navarro, Van Giai Nguyen and L. L. Salcedo, Ann. Phys. **214** (1992) 293.
- [16] T. Shigehara, K. Shimizu and A. Arima, Nucl. Phys. **A492** (1989) 388.
- [17] E. Bauer, A. Ramos and A. Polls, Phys. Rev. **C54** (1996) 2959.
- [18] E. Bauer and A. Lallena, Phys. Rev. C, *in press*.
- [19] C. Cób, K. F. Quader, R. D. Smith and J. Wambach; Nucl. Phys. **A485** (1988) 61.
- [20] S. Drozdż, S. Nishizaki, J. Speth and J. Wambach, Phys. Rep. **197** (1990) 1.
- [21] K. Takayanagi, K. Shimizu and A. Arima, Nucl. Phys. **A477** (1988) 205; K. Takayanagi, Phys. Lett. **230B** (1989) 11; Nucl. Phys. **A510** (1990) 162; Nucl. Phys. **A522** (1991) 494; Nucl. Phys. **A522** (1991) 523; Nucl. Phys. **A556** (1993) 14.
- [22] E. Bauer, Nucl. Phys. **A589** (1995) 669.
- [23] E. Bauer, A. Polls and A. Ramos, *in preparation*
- [24] Y. Horikawa, F. Lenz and Nimai C. Mukhopadhyay, Phys. Rev. **C22** (1980) 1680. C. R. Chinn, A. Picklesimer and J. W. Van Orden, Phys. Rev. **C40** (1989) 790. A. Picklesimer, J. W. Van Orden and S. J. Wallace, Phys. Rev. **C32** (1985) 1312. C. R. Chinn, A. Picklesimer and J. W. Van Orden, Phys. Rev. **C40** (1989) 1159. F. Capuzzi, C. Giusti and F. D. Pacati, Nucl. Phys. **A524** (1991) 681. F. Capuzzi, Nucl. Phys. **A554** (1993) 362.
- [25] W. M. Alberico, M. Ericson, A. Molinari and Zi-Xing Wang, Phys. Lett. **21B** (1989) 37.
- [26] M. Hjorth-Jorth-Jensen, M. Borromeo, H. Müther and A. Polls; Nucl. Phys. **A551** (1993) 580. M. Hjorth-Jorth-Jensen, H. Müther and A. Polls; Phys. Rev. **C50** (1994) 501.

- [27] R. Cenni, F. Conte and P. Saracco; Preprint GEF-TH-2/97.
- [28] E. Oset and L. L. Salcedo, Nucl. Phys. **A468** (1987) 631. R. C. Carrasco and E. Oset; Nucl. Phys. **A536** (1992) 445. J. Nieves, E. Oset and C. García-Recio; Nucl. Phys. **A554** (1993) 509 and Nucl. Phys. **A554** (1993) 554.
- [29] A. Gil, J. Nieves and E. Oset; Preprint FTUV/97-18.
- [30] B. Sommer, Nucl. Phys. **A308** (1978) 263.
- [31] G. E. Brown and W. Weise, Phys. Rep. **22** (1975) 279.
- [32] E. Shiino, Y. Saito, M. Ichimura and H. Toki, Phys. Rev. **C34** (1986) 1004.
- [33] A. Hosaka and H. Toki, Prog. Theor. Phys. **76** (1986) 1306.
- [34] C. F. Williamson, private communication.
- [35] I. S. Towner, Phys. Rep. **155** (1987) 263.

Figure Captions

Figure 1: Goldstone diagrams stemming from the free response (*Lind*) and the first order direct (exchange) *ph* term from the RPA series, designed by $(B_{1NN})_D$ ($(B_{1NN})_E$). In every diagram two wavy lines represent the external probe with momentum and energy \mathbf{q} and $\hbar\omega$, respectively. The dashed line represents the residual interaction. Only forward-going contributions are shown. We have assigned values to the momentum carried by each line.

Figure 2: Goldstone diagrams from contributions R_1 , R_{12} and R_2 (see Eqs. (27)-(29)). A dot between bubbles represents the sum of direct plus exchange contact interaction. Only some first order in V_1 and V_2 are shown. A double line represents the delta.

Figure 3: Goldstone diagrams stemming from Eq. (34). Bubbles with a straight line crossing in the middle represent the sum of direct and exchange first order in V_2 contributions.

Figure 4: Diagonal self energy insertions from Eq. (54). We show only some of the forward going second order contributions.

Figure 5: Some contributions from the non-diagonal self energy insertions to the structure function.

Figure 6: Intermediate Q -states over which the self energy is sum. Only direct terms are shown.

Figure 7: Exchange second orders self energy contributions with intermediate Q_1 configuration.

Figure 8: Comparison between the RA (continuous lines) and the sum of terms up to second order (dashed lines) for V_a (curve label (a)) and V_b (b) where the free structure function was subtracted from these curves and shown separately by dotted lines. Notation $R^*(q, \hbar\omega)$ indicates the structure function per unit volume. The energy is given in MeV and the structure function in units of $10^{-5} MeV^{-1} fm^{-3}$.

Figure 9: $R_{\Delta N}^*$ contribution to the structure function. The continuous line is our result, $B_{\Delta N}$. Non continuous lines represent the ΔN contribution from the RA. Long-dashed line is for $g'_{\Delta N} = 0.0$, dashed line for $g'_{\Delta N} = 0.3$, short dashed line for $g'_{\Delta N} = 0.43$ and dotted line for $g'_{\Delta N} = 0.6$. Units are the same as in Fig. 8.

Figure 10: RPA result for the structure function. In a), the continuous line is our result for the RPA with the delta. Dashed line is the RPA without the delta, while the dotted line is the free response. In b), we plotted γ as defined in Eq. (58); continuous and dashed lines has the same meaning as in a).

Figure 11: RPA result with the delta for two different values of $g'_{\Delta\Delta}$. In a), continuous line is for $g'_{\Delta\Delta} = 0.4$ and for dashed line $g'_{\Delta\Delta} = 0.6$. Dotted line is the free structure function. Figure b) has the same meaning as Fig. 10 b.

Figure 12: Comparison between the RPA and the RA approximations. Continuous lines is the RPA result for $g'_{\Delta\Delta} = 0.4$, dashed lines is the RPA result for $g'_{\Delta\Delta} = 0.6$; dotted dashed line is the RA result for $g'_{\Delta\Delta} = 0.4$ while double dotted-dashed line is the RA result for $g'_{\Delta\Delta} = 0.6$. The remainder parameters of the interaction are the ones of V_b . Dotted line is the free structure function.

Figure 13: Imaginary part of the self energy en MeV. The continuous line represents the Σ^{PQ_1P} contribution, the long dashed line is the Σ^{PQ_2P} one while the short dashed line is the Σ^{PQ_3P} contribution. In part a) of the figure, $P = P_N$ and in part b) $P = P_\Delta$. The interaction employed was V_c .

Figure 14: Imaginary part of the self energy $\Sigma^{\Delta Q_1 P_\Delta}$ en MeV. In both parts, a1) and b1) is our result for $g'_{\Delta N} = 0.6$, $\Lambda_{\pi\Delta N} = \Lambda_{\rho\Delta N} = 1000$ MeV/c. While all other parameters are the ones of V_c . All a1) has the same cut offs while $g'_{\Delta N}$ is changed: 0.6 for a2) and 0.4 for a3). And also, all b1) curves has the same $g'_{\Delta N}$ value and different cut offs: $\Lambda_{\pi\Delta N} = \Lambda_{\rho\Delta N} = 850$ MeV/c for b2), $\Lambda_{\pi\Delta N} = \Lambda_{\rho\Delta N} = 1200$ MeV/c for b3) and for b4) $\Lambda_{\pi\Delta N} = 850$ MeV/c and $\Lambda_{\rho\Delta N} = 1200$ MeV/c.

Figure 15: Non diagonal self energy contributions to the structure function. Dashed line is the sum of graphs without the delta and the continuous line includes it. Also we show γ as in Eq. (58) but where the RPA response was replaced by the non diagonal self energy contribution.

Figure 16: Final result for the structure function with self energies insertions. The dotted line is the free response. The continuous line is the response function per unit volume with the Σ^{PQ_1P} self energy insertion. The dashed line includes all self energy insertions. Dotted line is the free structure function.

Figure 17: Transverse response function for ^{40}Ca at momentum transfer $q = 410$ MeV/c for *a*) and $q = 550$ MeV/c for *b*), in units of $10^{-3} MeV^{-1}$. Dotted lines is the free response. Continuous line is our result from Eq. (56) for the V_c interaction. Dashed line is our result where the delta was excluded. Data was taken from [3] (circles) and [34] (triangles).

Figure 18: Direct plus exchange graphs needed to evaluate $g'_{1\Delta\Delta}$.

V	g'_{NN}	g_{NN}	$g'_{\Delta N}$	$g'_{\Delta\Delta}$
V_a	0.5	0.0	0.0	0.3
V_b	0.7	0.3	0.0	0.5
V_c	0.7	0.3	0.6	0.4

Table I: Values of the Landau Migdal parameters entering in the different interactions employed in the text.

B_{1NN}			
V	$\hbar\omega$	<i>dir.</i>	<i>exc.</i>
V_a	40.	-8.17	2.36
	150.	3.38	-1.12
V_b	40.	-18.90	5.68
	150.	7.84	-2.48

$B_{1\Delta\Delta}$			
V	$\hbar\omega$	<i>dir.</i>	<i>exc.</i>
V_a	320.	-21.45	5.51
	400.	20.83	-5.35
V_b	320.	-41.21	67.25
	400.	40.04	-58.91

Table II: Direct and exchange first order contributions from the RPA series to the structure function at momentum transfer $q = 410 \text{ MeV}/c$. The residual interaction is taken from Table I. We have considered the NN and $\Delta\Delta$ channels. The energy is given in MeV and the structure function in units of $10^{-5} \text{ MeV}^{-1} \text{ fm}^{-3}$. The values of the energy where taken closer to the points where each particular response has its extreme.

$B_{1\Delta N}$				
V	$\hbar\omega$	<i>dir.</i>	<i>exc.</i>	<i>exc (w.t.)</i>
V_a	100.	4.37	-8.30	-1.99
	340.	-1.55	3.01	0.79

$B_{2\Delta N}$				
V	$\hbar\omega$	<i>dir.</i>	<i>exc.</i>	<i>exc (w.t.)</i>
V_a	50.	-1.22	1.69	0.57
	100.	-0.78	2.05	0.54
	320.	1.25	-3.90	-0.99
	400.	-0.75	2.34	0.55

Table III: The same as Table II, but for the ΔN channel. We have also included second order contributions $B_{2\Delta N}$. In the last column *exc(w.t.)*, we have shown the exchange term without the tensor contribution to the residual interaction.

$Im \Sigma^{P_N Q_1 P_N}$		
$\hbar\omega$	dir.	exc.
100.	-13.31	0.20
200.	-19.46	1.12
300.	-16.34	0.83
400.	-13.12	0.23

$Im \Sigma^{P_\Delta Q_1 P_\Delta}$		
$\hbar\omega$	dir.	exc.
100.	-17.14	0.80
200.	-28.85	3.08
300.	-28.92	1.89
400.	-26.98	0.63

Table IV: Direct and exchange self energy contributions in units of MeV for several energies.

Lind

$(B_{1\text{ }NN})_D$

$(B_{1\text{ }NN})_E$

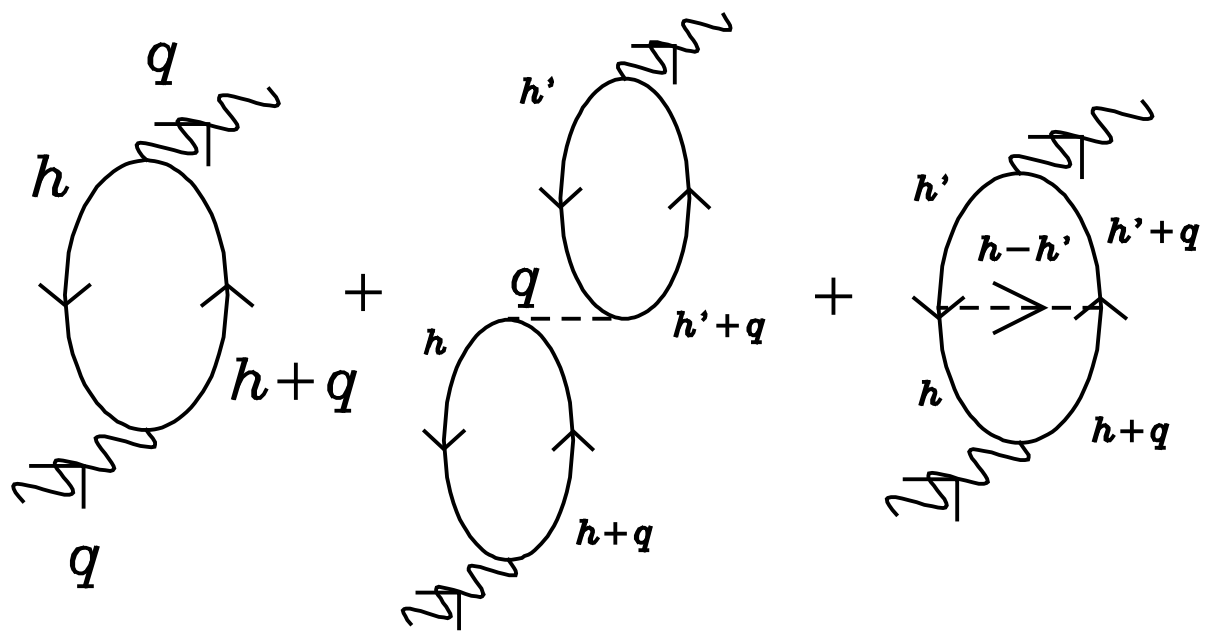


Fig. 1.

$$R_1 = \text{Diagram 1} + \text{Diagram 2} + \text{Diagram 3} + \text{Diagram 4} + \dots$$

$$R_{12} = \text{Diagram 1} - \text{Diagram 2} + \text{Diagram 3} - \text{Diagram 4} + \dots$$

$$+ \text{Diagram 5} - \text{Diagram 6} + \dots$$

$$R_2 = \text{Diagram 1} - \text{Diagram 2} + \text{Diagram 3} - \text{Diagram 4} + \dots$$

Fig. 2.

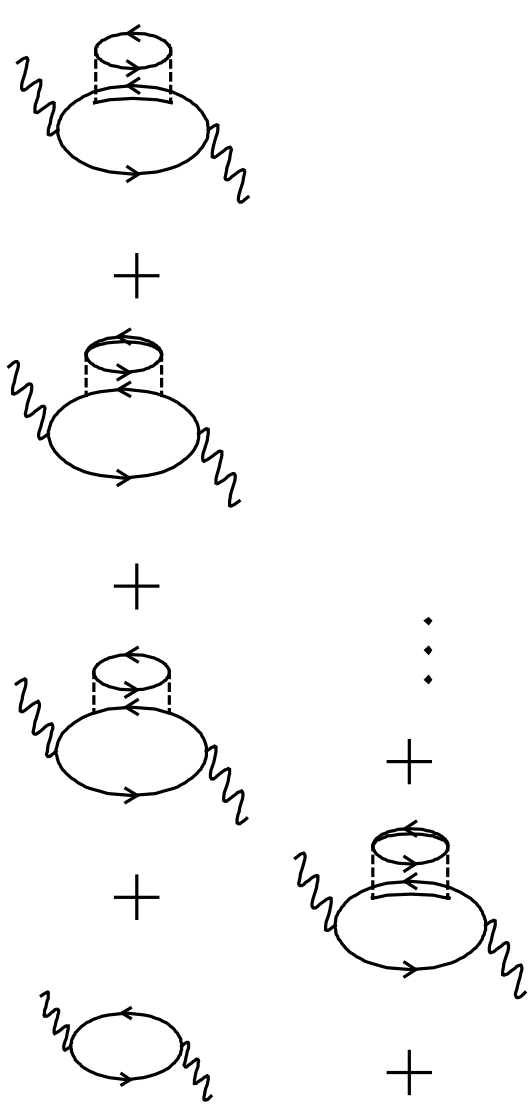
$$(R_{12})_{NN} =$$

$$(R_{12})_{\Delta\Delta} =$$

$$(R_{12})_{\Delta N} =$$

Fig. 3.

$$(R_{NN}^{L+SE})^{diag.} =$$



$$(R_{\Delta\Delta}^{L+SE})^{diag.} =$$

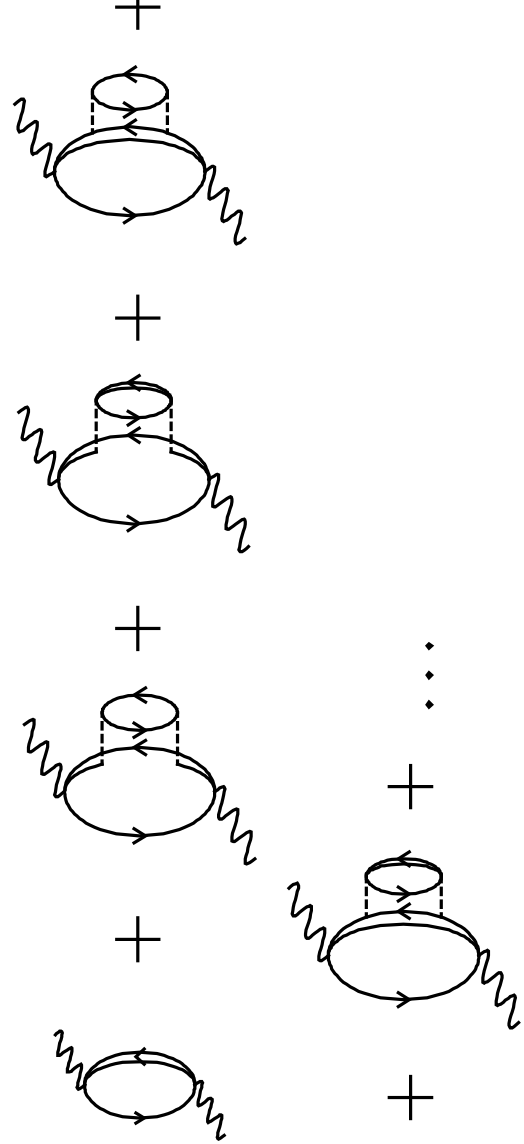


Fig. 4.

$$(R_{PP}^{SE})^{non\ diag.} =$$

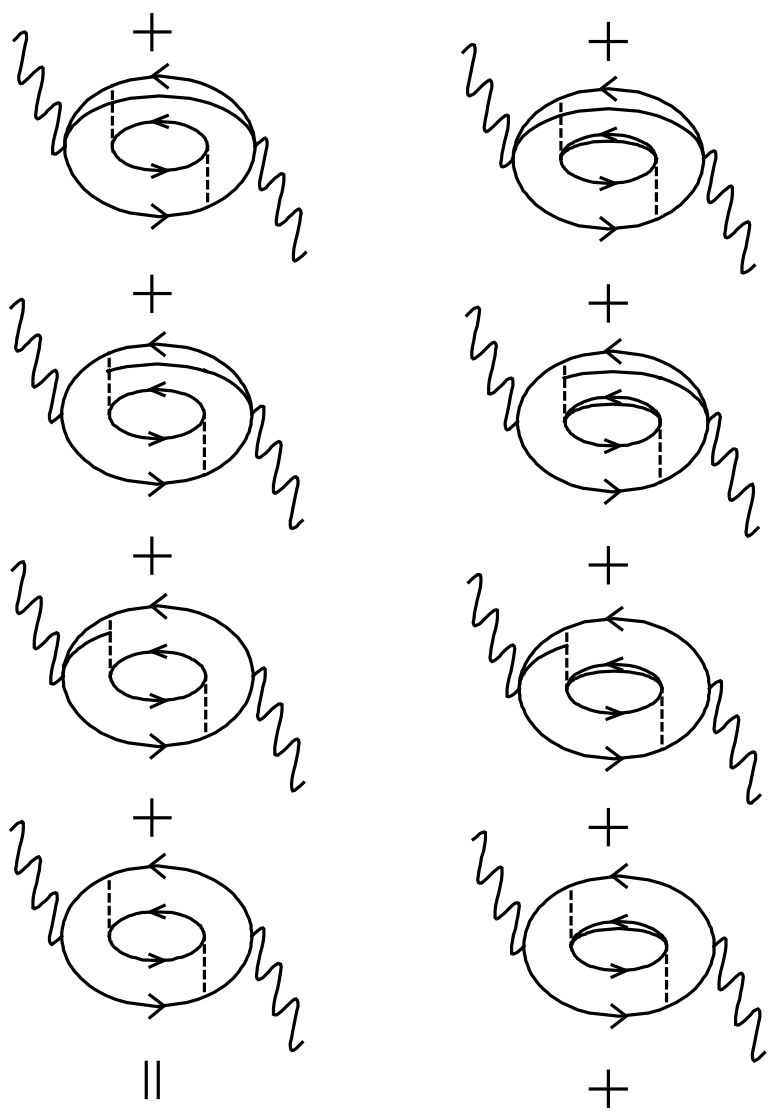


Fig. 5.

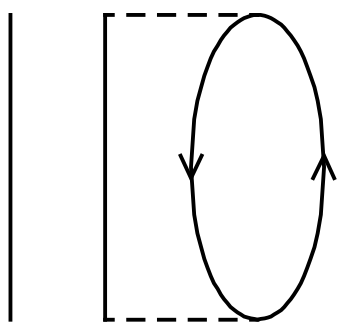
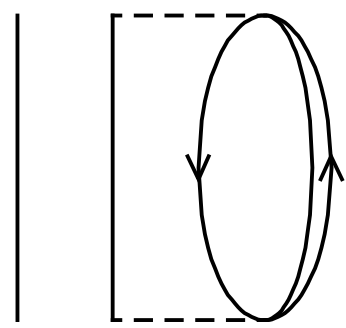
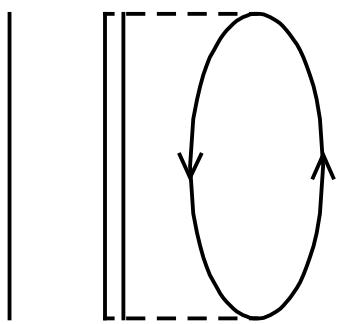
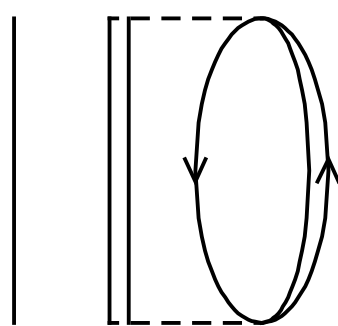
Q_1  Q_2  Q_3  Q_4 

Fig. 6.

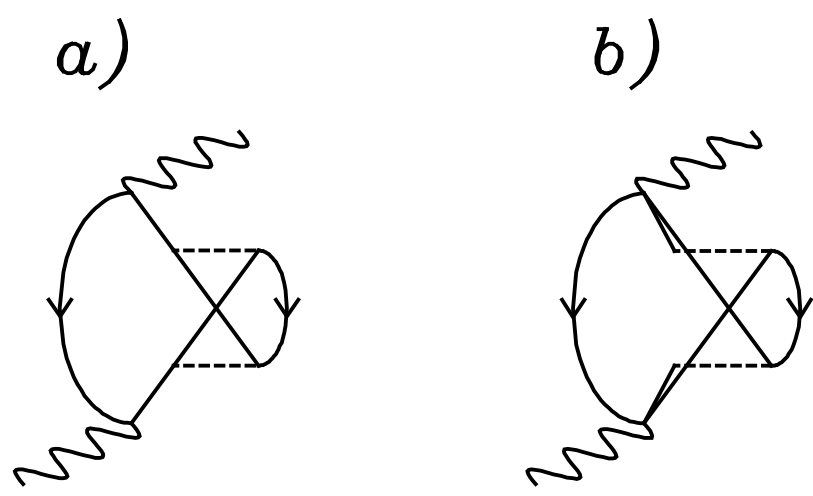


Fig. 7.

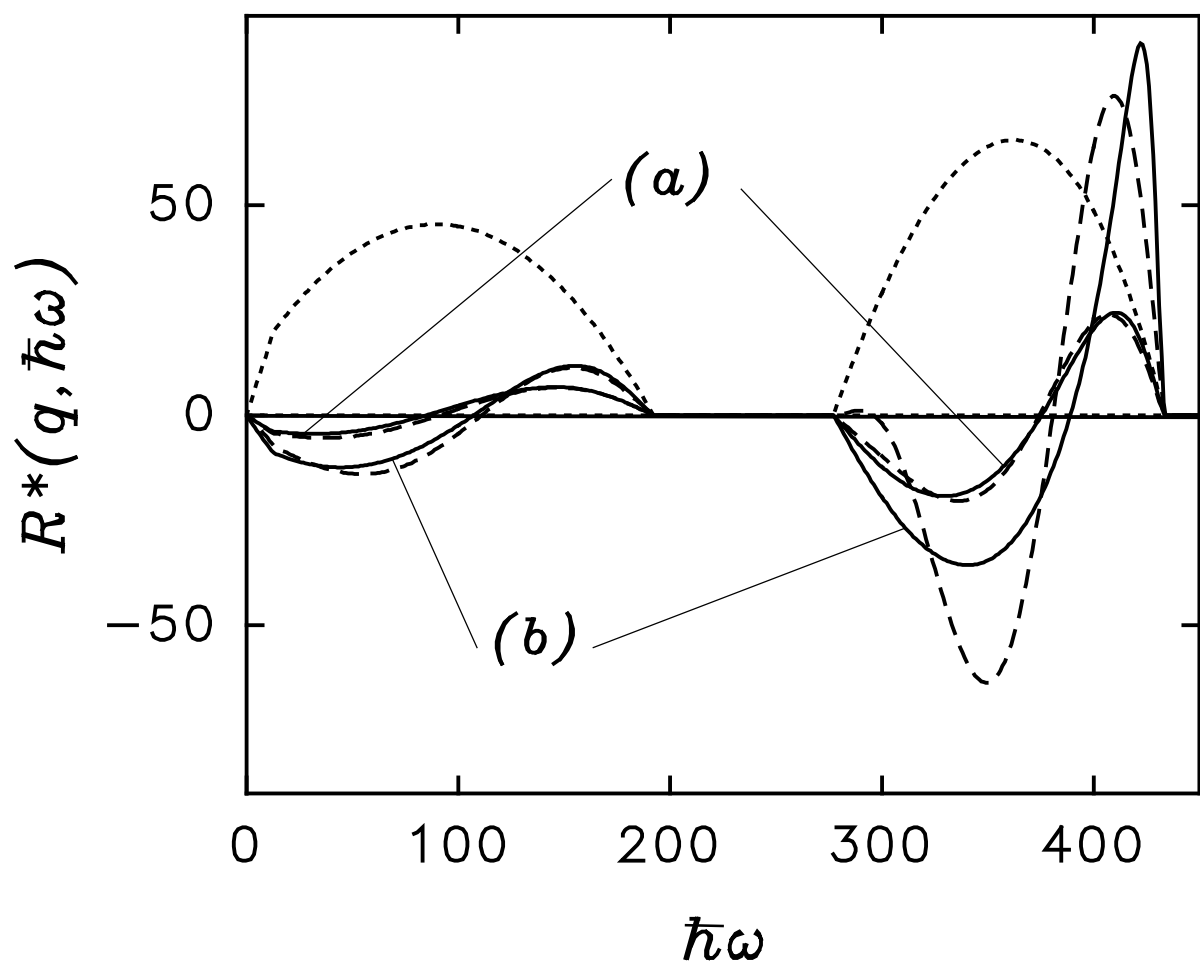


Fig. 8.

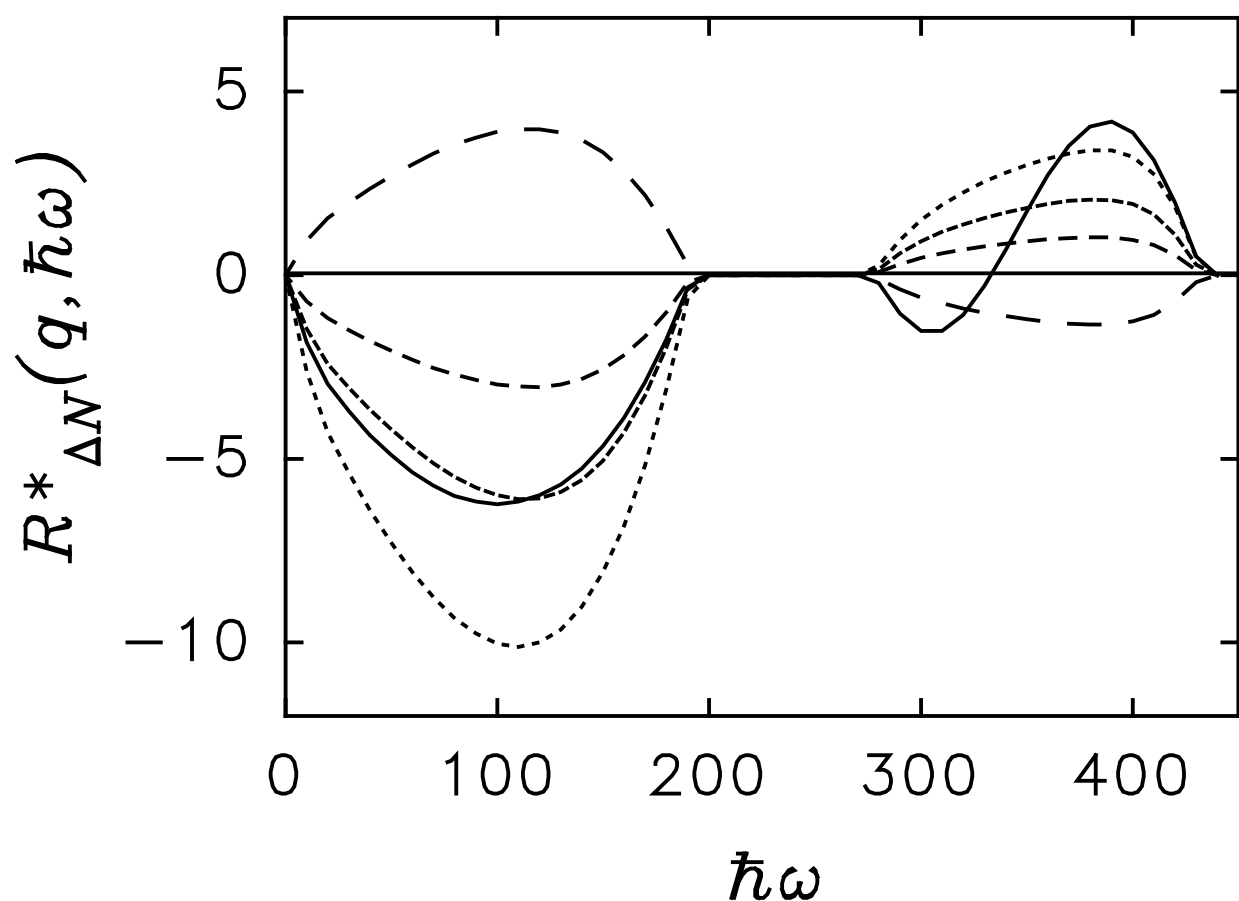


Fig. 9.

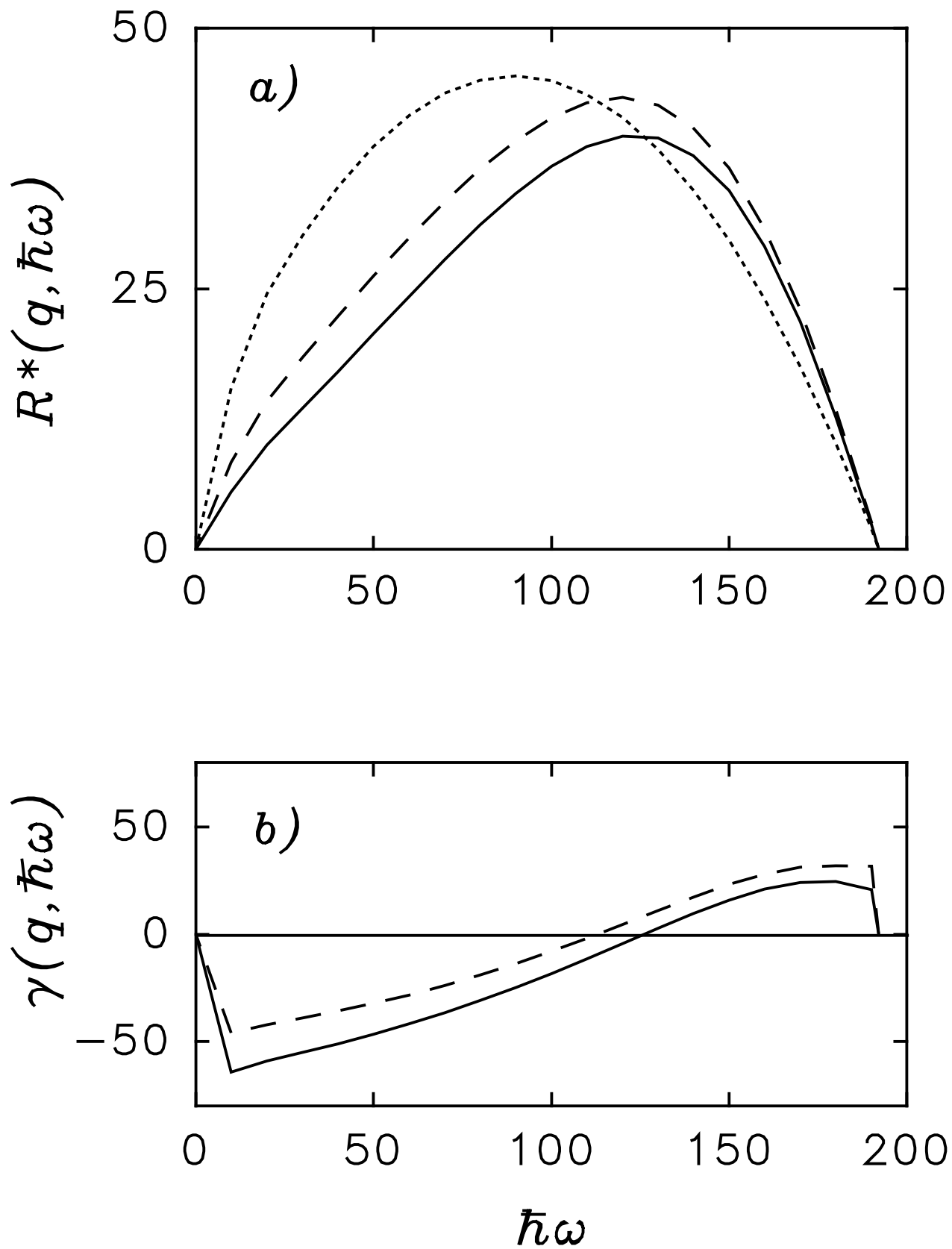


Fig. 10.

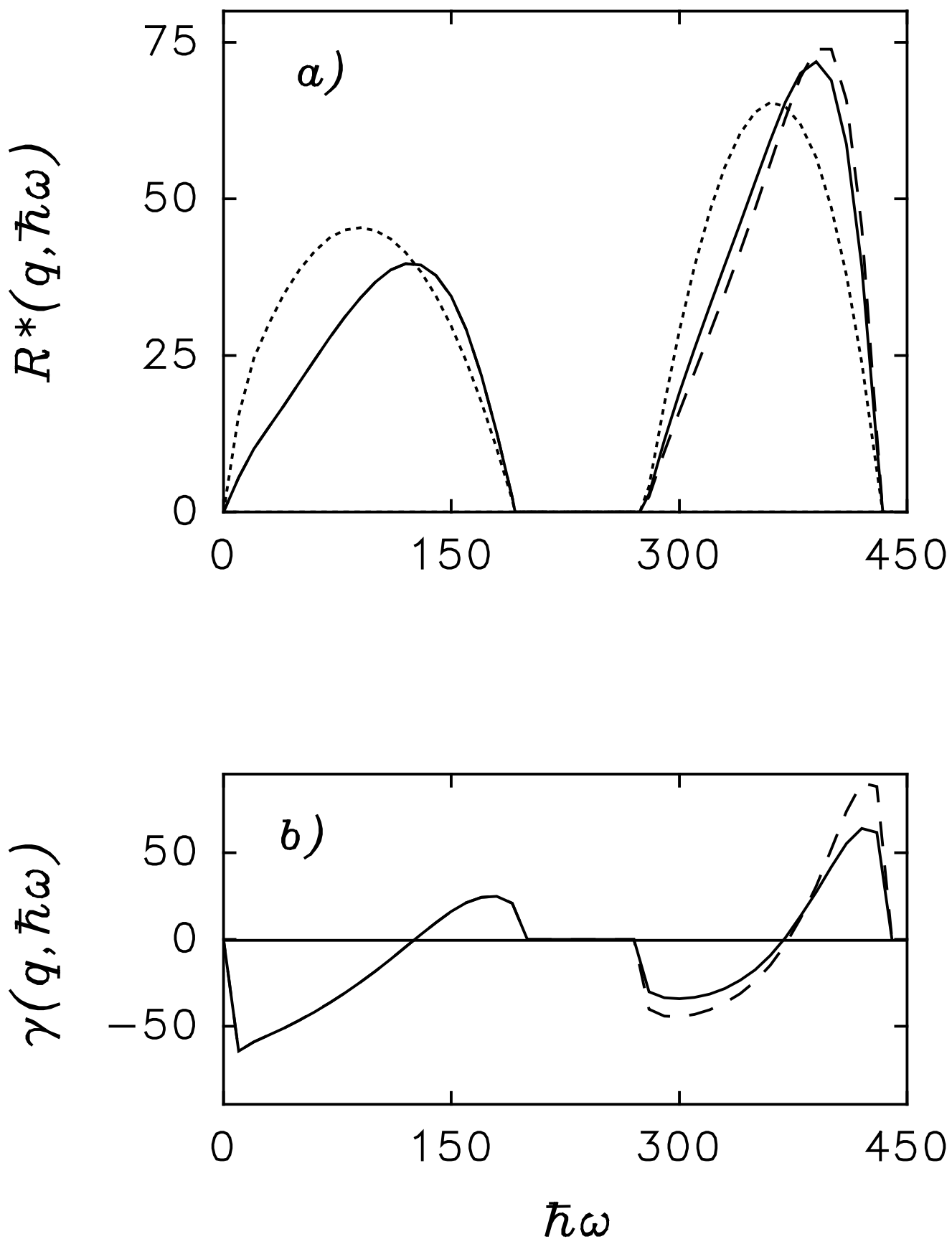


Fig. 11.

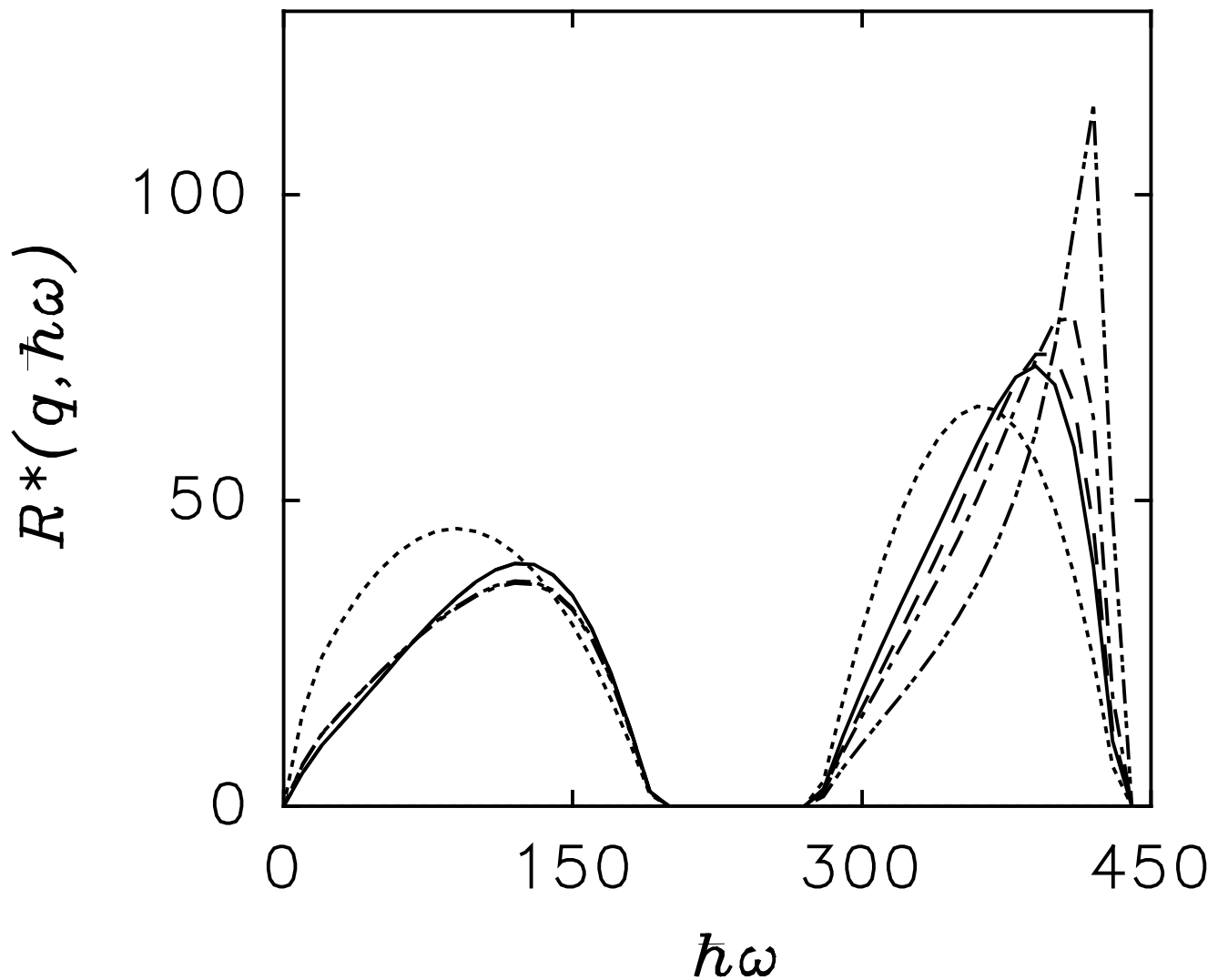


Fig. 12.

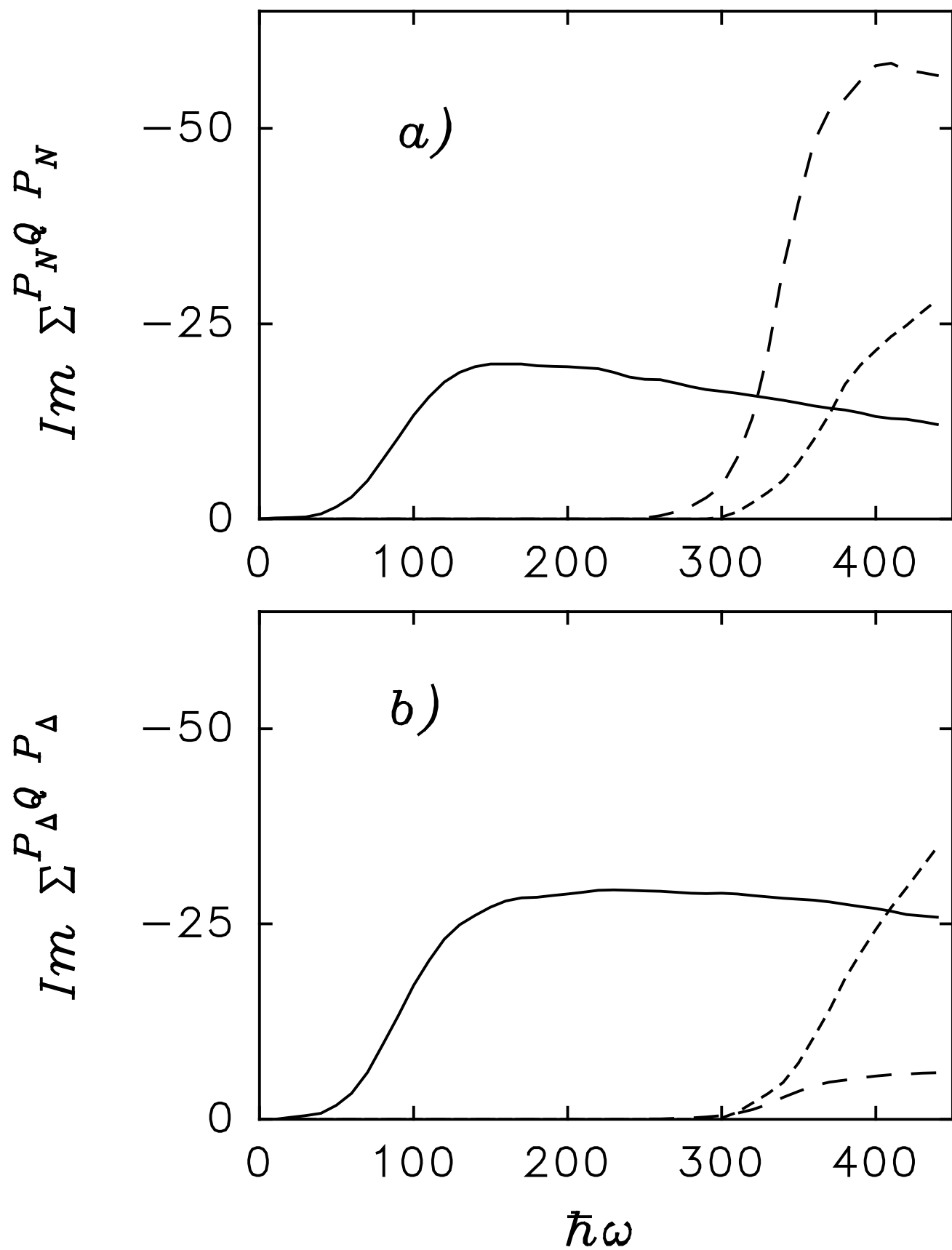


Fig. 13.

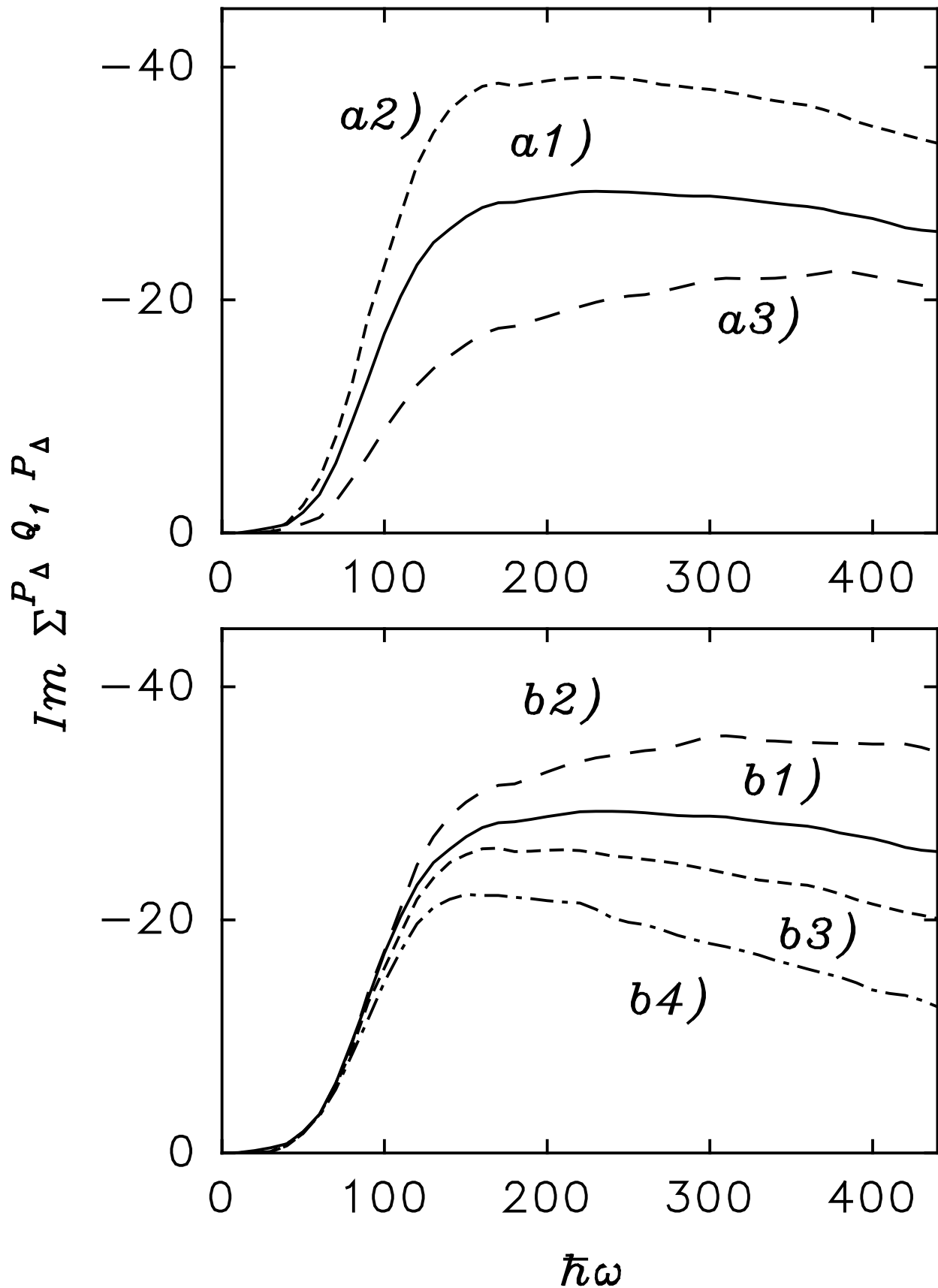


Fig. 14.

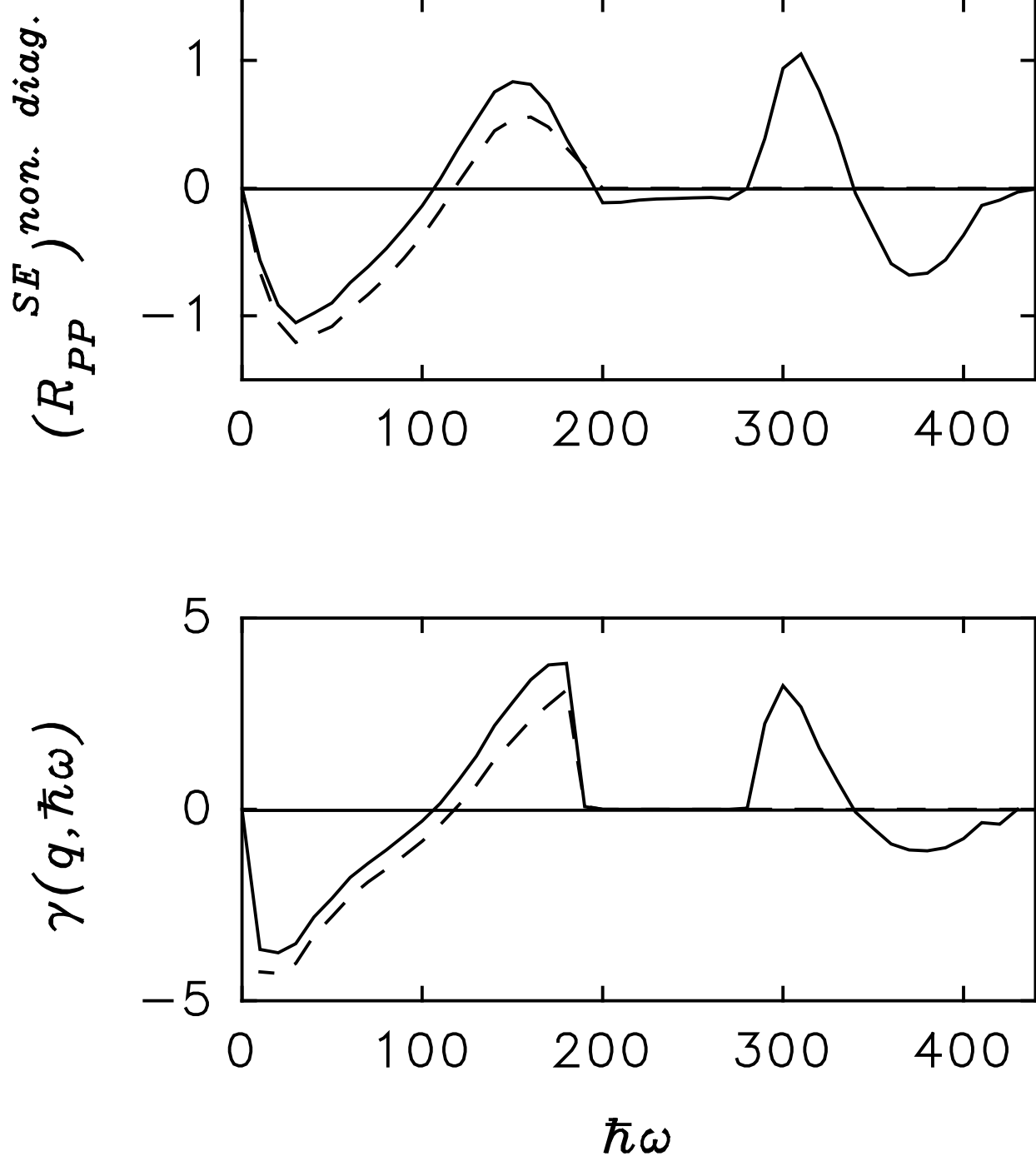


Fig. 15.

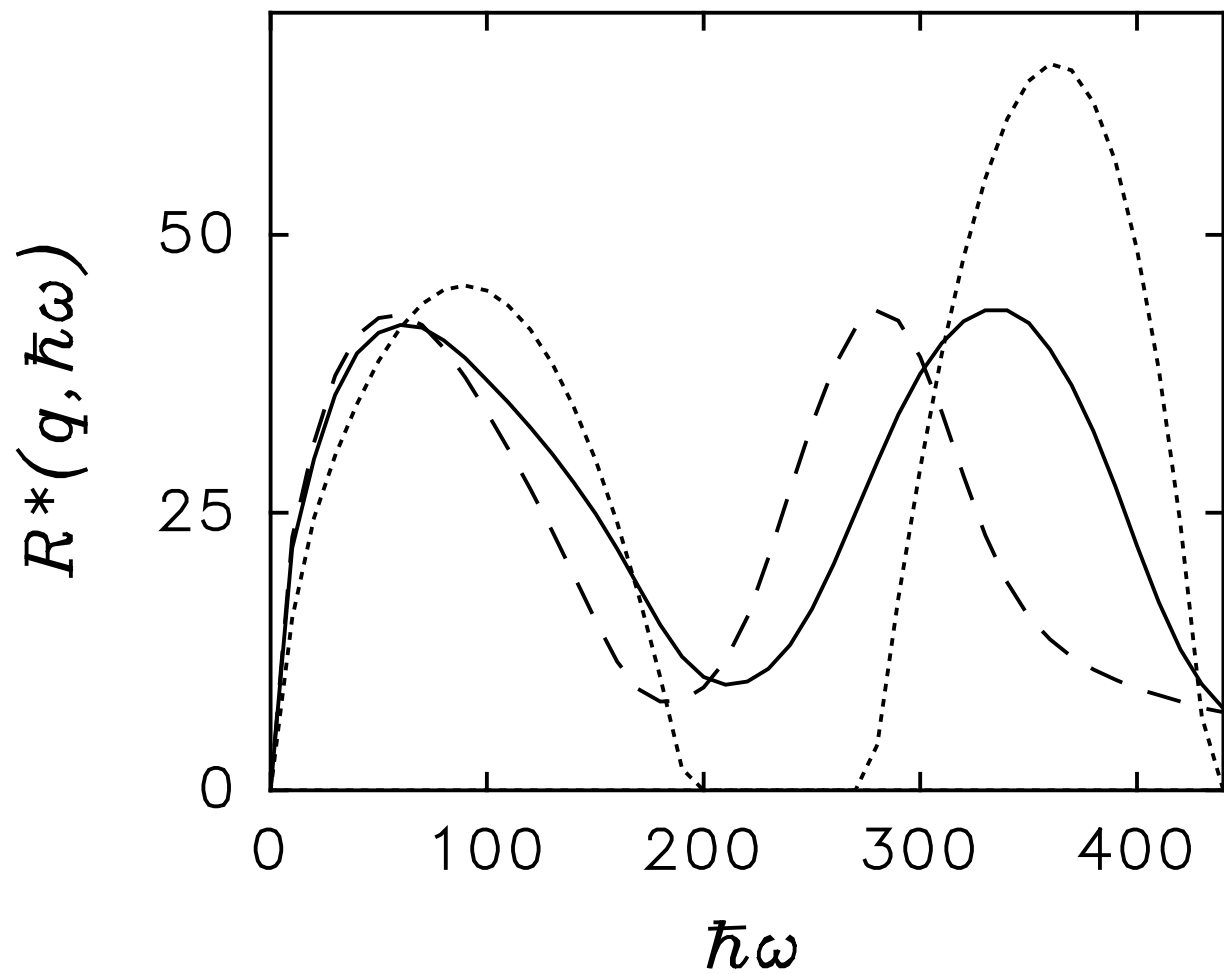


Fig. 16.

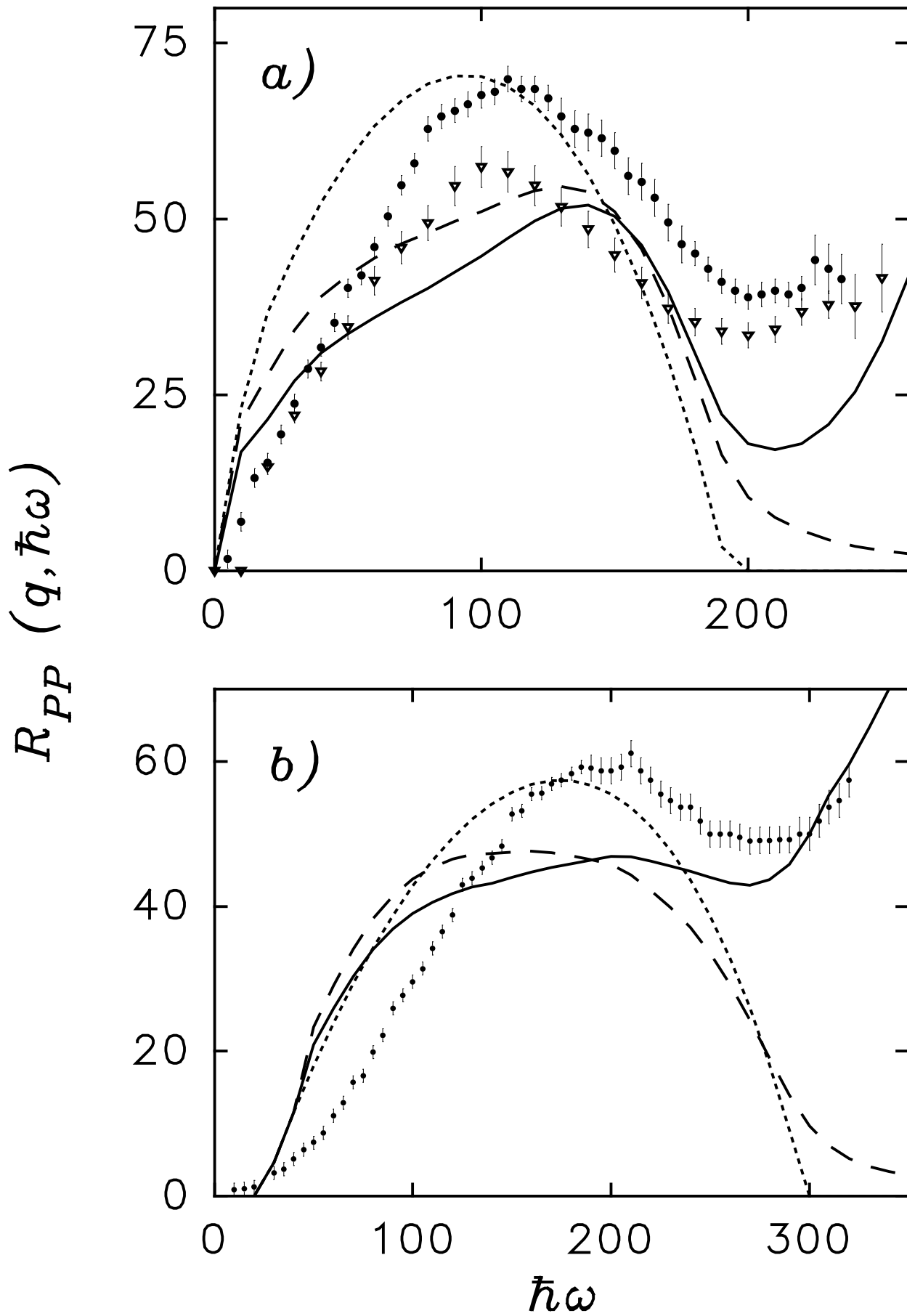


Fig. 17.

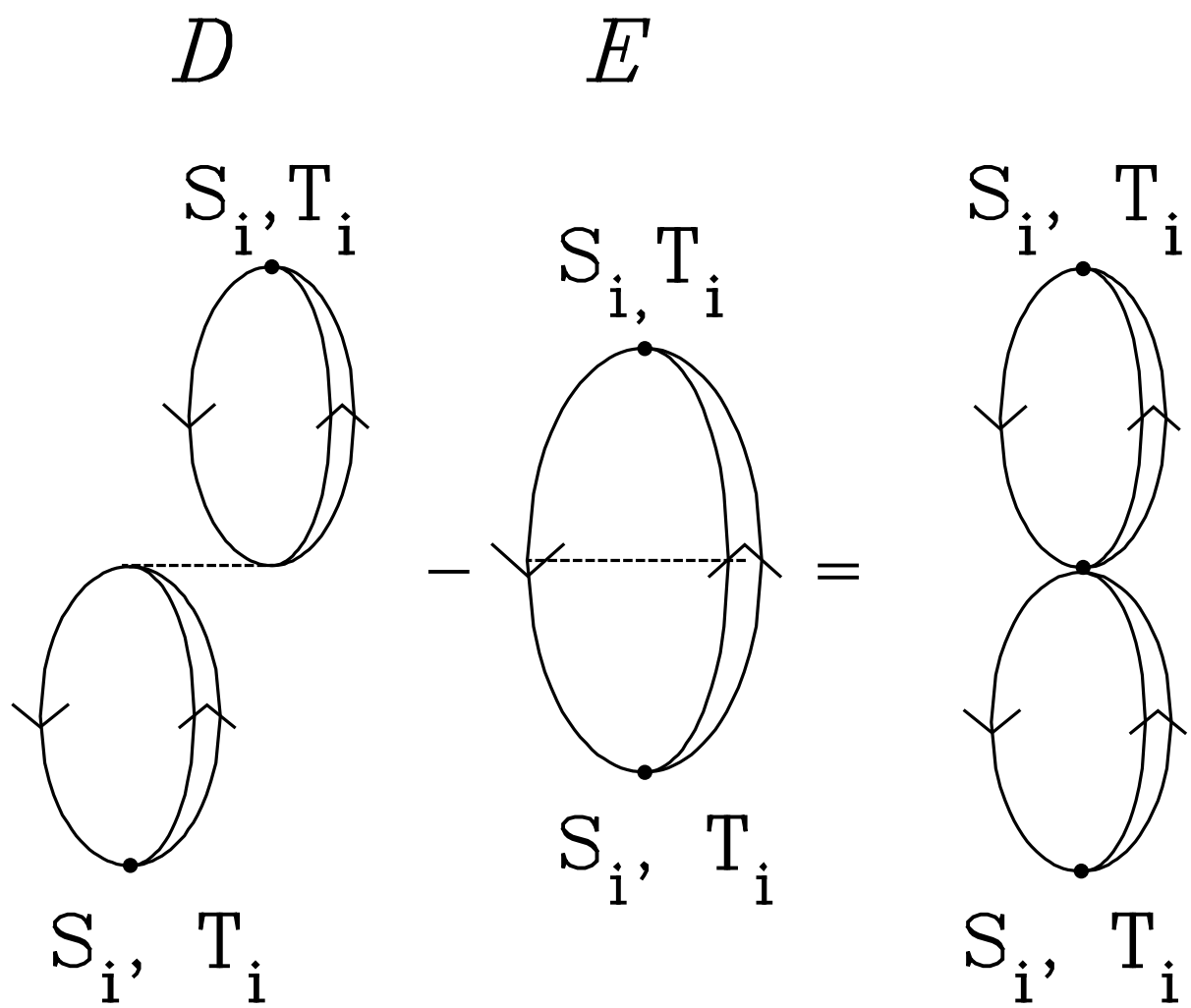


Fig. 18.